Inorg. Chem. **2002**, *41*, 3990–4005

Alkyl and Aryl Substituted Corroles. 3. Reactions of Cofacial Cobalt Biscorroles and Porphyrin-Corroles with Pyridine and Carbon Monoxide

Karl M. Kadish,*,† Zhongping Ou,† Jianguo Shao,† Claude P. Gros,‡ Jean-Michel Barbe,‡ François Jérôme,‡ Frédéric Bolze,‡ Fabien Burdet,‡ and Roger Guilard*,‡

Department of Chemistry, University of Houston, Houston, Texas 77204-5003, and Université de Bourgogne, LIMSAG UMR 5633, Faculté des Sciences Gabriel, 6, boulevard Gabriel, 21000 - Dijon, France

Received January 22, 2002

The synthesis and characterization of three new cofacial biscorroles and three new linked Co(II) porphyrins and Co(III) corroles with the same face to face orientation are described. The biscorroles are represented as (BCS)Co_2, (BCO)Co_2, (BCX)Co_2 while the porphyrin-corrole dyads are represented as (PCA)Co_2, (PCB)Co_2, (PCO)Co_2 where BC represents the Co(III) cofacial biscorroles and PC represents the porphyrin-corrole complexes which are linked to each other by a dibenzothiophene (S), dibenzofuran (O), or 9,9-dimethylxanthene (X) bridge in the case of the corroles and an anthracene (A), biphenylene (B), or dibenzofuran (O) bridge in the case of the mixed macrocycle derivatives. The electrochemical and spectroscopic data on these new bismacrocycles are compared to those of previously reported biscorroles of the type (BCA)Co_2 and (BCB)Co_2. The CO and/or pyridine binding properties of each biscorrole and porphyrin-corrole in CH_2Cl_2 are also presented. Only one CO ligand is bound axially to each corrole unit of the bismacrocycle but five- and six-coordinate pyridine complexes can be generated for the same compounds, with the exact stoichiometry depending upon the concentration of pyridine in solution. In all cases, the six-coordinate bispyridine corrole complex can be unambiguously identified by a strong diagnostic marker band located at 598–601 nm. The formation constants for pyridine binding to the biscorroles range from log $K_1 = 3.14$ to 5.08 while log K_2 ranges from 1.10 to 2.61 depending upon the specific spacer. Carbon monoxide binding constants range from log $K = 3.6$ to 4.0 in the case of the biscorroles and from log $K = 3.4$ to 4.1 in the case of the porphyrin-corrole dyads. These values also depend on the specific spacer in the complex and, like the pyridine binding constants, decrease in the order BCO > BCA > BCB for the biscorroles and PCO > PCA > PCB for the porphyrin-corrole complexes.

Introduction

A number of cofacial bisporphyrins have been synthesized and investigated as to their reactivity with small molecules over the last 25 years. The examined compounds include bisporphyrins linked by two or more flexible strapping units[1−7] as well as pillared bisporphyrins linked via a single rigid spacer.[1,8−13] Spacers investigated in the latter group include anthracene and biphenylene moieties, and the dibenzofuran and xanthene groups recently reported by Nocera and co-workers.[10,12]

* To whom correspondence should be addressed. E-mail: KKADISH@UH.EDU (K.K.); roger.guilard@u-bourgogne.fr (R.G.).
† University of Houston.
‡ Université de Bourgogne.

(1) Collman, J. P.; Wagenknecht, P. S.; Hutchison, J. E. *Angew. Chem., Int. Ed. Engl.* **1994**, *33*, 1537−1554.
(2) Chang, C. K.; Kuo, M. S.; Wang, C. B. *J. Heterocycl. Chem.* **1977**, *14*, 943−945.
(3) Collman, J. P.; Elliot, C. M.; Halbert, T. R.; Tovrog, B. S. *Proc. Natl. Acad. Sci. U.S.A.* **1977**, *74*, 18−22.
(4) Cowan, J. A.; Sanders, J. K. M. *J. Chem. Soc., Chem. Commun.* **1985**, 1213−1214.
(5) Kagan, N. E.; Mauzerall, D.; Merrifield, R. B. *J. Am. Chem. Soc.* **1984**, *99*, 5484−5486.
(6) Karaman, R.; Almarsson, O.; Bruice, T. C. *J. Org. Chem.* **1992**, *57*, 1555−1559.
(7) Ogoshi, H.; Sugimoto, H.; Yoshida, Z. *Tetrahedron Lett.* **1977**, 169−172.
(8) Chang, C. K.; Abdalmuhdi, I. *J. Org. Chem.* **1983**, *48*, 5388−5390.
(9) Chang, C. K.; Abdalmuhdi, I. *Angew. Chem., Int. Ed. Engl.* **1984**, *23*, 164−165.
(10) Chang, C. J.; Deng, Y.; Heyduk, A. F.; Chang, C. K.; Nocera, D. G. *Inorg. Chem.* **2000**, *39*, 959−966.
(11) Clement, T. E.; Nurco, D. J.; Smith, K. M. *Inorg. Chem.* **1998**, *37*, 1150−1160.
(12) Deng, Y.; Chang, C. J.; Nocera, D. G. *J. Am. Chem. Soc.* **2000**, *122*, 410−411.
(13) Harriman, A.; Sauvage, J. P. *Chem. Soc. Rev.* **1996**, *25*, 41−49.

10.1021/ic020058+ CCC: $22.00
Published on Web 06/27/2002

Scheme 1

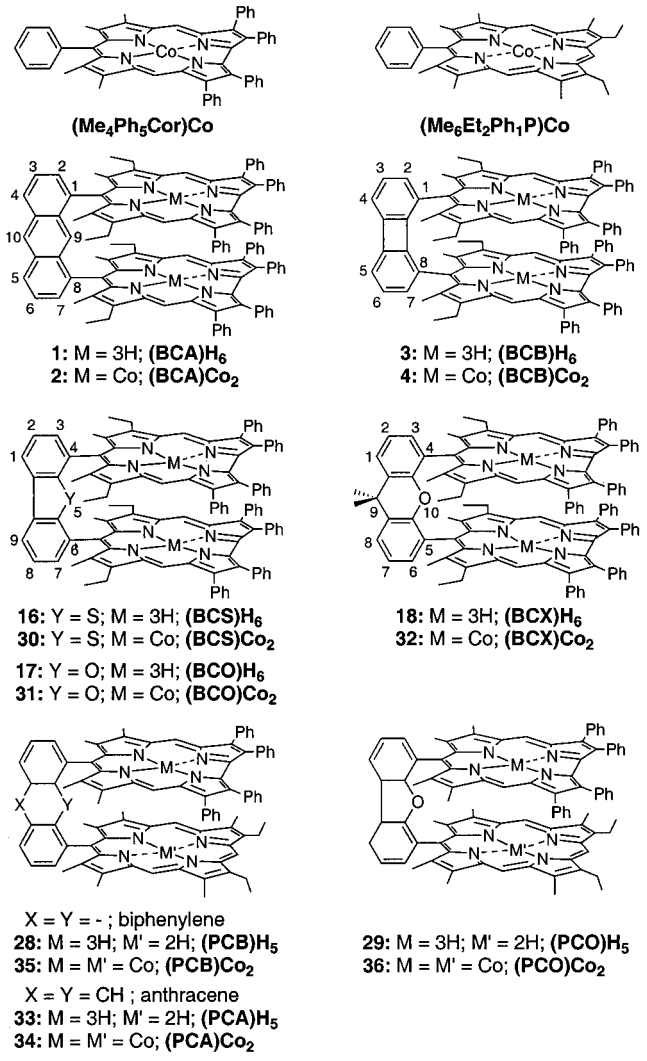

Studies of cofacial biscorroles possessing spacers similar to those in the pillared porphyrin series of compounds have also attracted much attention in recent years, both because of the chemical and structural similarities between corroles and the porphyrins and the fact that corroles can generally stabilize the central metal ions in higher oxidation states.[14] Our own laboratories recently reported the synthesis, electrochemistry, and axial ligand binding properties of six cobalt monocorroles containing different meso or β-pyrrole substituents[15] and two cofacial cobalt biscorroles possessing the same macrocycle and an anthracenyl or a biphenylenyl bridge.[16] These latter two compounds are represented as $(BCA)Co_2$ and $(BCB)Co_2$ where BC represents the biscorrole and A or B represents the anthracene or biphenylene bridge, respectively.[16]

In this present paper, we report the synthesis, electrochemistry, and spectroscopic characterization of additional cofacial biscorroles with dibenzothiophene, dibenzofuran, or 9,9-dimethylxanthene bridges whose structures are shown in Scheme 1. The pyridine and carbon monoxide binding properties of the cobalt biscorroles are also presented, and these data are then compared to those for previously characterized $(BCA)Co_2$ and $(BCB)Co_2$ as well as the analogous monocorrole in order to better understand how the ligand binding properties of these biscorrole complexes might be modified by the bridge which links the two macrocycles in a face to face orientation.

We also report in this paper the synthesis and characterization of three porphyrin-corrole dyads with bridging anthracene, biphenylene, or dibenzofuran. The structures of these compounds are also shown in Scheme 1. Carbon monoxide and pyridine binding properties of these three compounds, represented as $(PCA)Co_2$ (A = anthracene),[17] $(PCB)Co_2$ (B = biphenylene), and $(PCO)Co_2$ (O = dibenzofuran) are also examined. From an analysis of these data, we thus can better understand how the type of porphyrin or corrole complex affects the ligand binding and electrochemical properties of the cobalt corrole in a bismacrocycle unit containing either two cobalt(III) corroles or one cobalt(III) corrole and one cobalt(II) porphyrin.

Experimental Section

Instrumentation. ^{1}H NMR spectra were recorded on a Bruker AC 200 Fourier or Bruker DRX-500 AVANCE transform spectrometer at the Centre de Spectrométrie Moléculaire de l'Université de Bourgogne; chemical shifts are expressed in ppm relative to chloroform (7.258 ppm) or benzene (7.15 ppm). Microanalyses were performed at the Université de Bourgogne on a Fisons EA 1108 CHNS instrument. IR spectra were recorded on a Bruker IFS 66v FTIR spectrophotometer, and samples were prepared as 1% dispersion in KBr pellets. UV−vis spectra were recorded on a Varian Cary 1 spectrophotometer. Mass spectra were obtained with a Kratos Concept 32 S spectrometer in the EIMS or LSIMS modes or on a Bruker ProFLEX III spectrometer in the MALDI/TOF mode using dithranol as a matrix. Cyclic voltammetry was carried out with an EG&G model 173 potentiostat. A three-electrode system was used and consisted of a glassy carbon or platinum disk working electrode, a platinum wire counter electrode, and a saturated calomel reference electrode (SCE). The SCE was separated from the bulk of the solution by a fritted-glass bridge of low porosity which contained the solvent/supporting electrolyte mixture. Half wave potentials were calculated as $E_{1/2} = (E_{pa} + E_{pc})/2$ and are referenced to the SCE.

UV−vis spectroelectrochemical experiments were performed with an optically transparent platinum thin-layer electrode of the type described in the literature.[18] Potentials were applied with an EG&G model 173 potentiostat. Time-resolved UV−vis spectra were recorded with a Hewlett-Packard model 8453 diode array rapid-scanning spectrophotometer. Infrared spectra were recorded on an FTIR Nicolet Magna-IR 550 spectrometer. The background was obtained by recording the IR spectrum of CH_2Cl_2 saturated with N_2, and the IR spectrum of the compound under CO was obtained after bubbling CO through the solution for 10−15 min.

(14) (a) Erben, C.; Will, S.; Kadish, K. M. In *The Porphyrin Handbook*; Kadish, K. M., Smith, K. M., Guilard, R., Eds.; Academic Press: San Diego, CA, 2000, Vol. 2, p 233−300. (b) Paolesse, R. In *The Porphyrin Handbook*; Kadish, K. M., Smith, K. M., Guilard, R., Eds.; Academic Press: San Diego, CA, 2000; Vol. 2, p 201−232.
(15) Guilard, R.; Gros, C. P.; Bolze, F.; Jérôme, F.; Ou, Z.; Shao, J.; Fischer, J.; Weiss, R.; Kadish, K. M. *Inorg. Chem.* **2001**, *40*, 4845−4855.
(16) Guilard, R.; Jérôme, F.; Barbe, J.-M.; Gros, C. P.; Ou, Z.; Shao, J.; Fischer, J.; Weiss, R.; Kadish, K. M. *Inorg. Chem.* **2001**, *40*, 4856−4865.
(17) Guilard, R.; Jérôme, F.; Gros, C. P.; Barbe, J.-M.; Ou, Z.; Shao, J.; Kadish, K. M. *C. R. Acad. Sci., Ser. IIc: Chim.* **2001**, *4*, 245−254.
(18) Lin, X. Q.; Kadish, K. M. *Anal. Chem.* **1985**, *57*, 1498−1501.

Chemicals and Reagents. Absolute dichloromethane (CH_2Cl_2) and pyridine (py) were obtained from Fluka Chemical Co. and used as received. Benzonitrile (PhCN) was purchased from Aldrich Chemical Co. and distilled over P_2O_5 under vacuum prior to use. Neutral alumina (Merck; usually Brockmann Grade III, i.e., deactivated with 6% water) and silica gel (Merck; 70−120 mm) were used for column chromatography. Analytical thin-layer chromatography was performed using Merck 60 F254 silica gel (precoated sheets, 0.2 mm thick). Reactions were monitored by thin-layer chromatography and UV−vis spectrometry. Tetra-*n*-butylammonium perchlorate (TBAP, Fluka Chemical Co.) was twice recrystallized from absolute ethanol and dried in a vacuum oven at 40 °C for a week prior to use.

Ethyl 3-ethyl-4-methyl-1*H*-pyrrole-2-carboxylate **(8)**,[19,20] ethyl 3,4-dimethyl-1*H*-pyrrole-2-carboxylate **(21)**,[19,20] 3,4-diphenyl-2-formylpyrrole **(15)**,[17,21−23] 4,6-diformyldibenzofuran **(6)**,[10,12,24] 4,5-diformyl-9,9-dimethylxanthene **(7)**,[10,12,24] 4,6-bis-(5,5′-ethoxycarbonyl-4,4′-diethyl-3,3′-dimethyldipyrromethan-5-yl)dibenzofuran **(10)**,[10,12,24] 4,5-bis-(5,5′-ethoxycarbonyl-4,4′-diethyl-3,3′-dimethyldipyrromethan-5-yl)-9,9-dimethylxanthene **(11)**,[10,12,24] 4,6-bis-(4,4′-diethyl-3,3′-dimethyldipyrromethan-5-yl)dibenzofuran **(13)**,[10,12,24] 4,5-bis-(4,4′-diethyl-3,3′-dimethyldipyrromethan-5-yl)-9,9-dimethylxanthene **(14)**,[10,12,24] 1-(2,3,7,8,12,18-hexamethyl-13,17-diethylporphyrin-5-yl)-8-(2,3,17,18-tetraethyl-7,8,12,13-tetramethylcorrol-10-yl)anthracene **(33)**,[17,22,23] and 1-(cobalt(II)-2,3,7,8,12,18-hexamethyl-13,17-diethylporphyrin-5-yl)-8-(cobalt(III)-2,3,17,18-tetraphenyl-7,8,12,13-tetramethylcorrol-10-yl)anthracene **(34)**[17,22,23] have been synthesized as already described.

4,6-Diformyl-dibenzothiophene (5). Dibenzothiophene (4.20 g, 25 mmol) was dissolved under argon in 125 mL of heptane. *N*,*N*,*N*′,*N*′-Tetramethylethylenediamine (TMEDA) (10 mL) was added after which the solution was deaereted by bubbling argon for 10 min. *n*-Butyllithium (1.6 M) in *n*-hexane (40 mL, 64 mmol) was added dropwise, and the mixture was heated to reflux for 15 min. The mixture was cooled to room temperature and then to 0 °C (ice bath). Dry DMF (10 mL, 128 mmol), freshly distilled over CaH_2, was added dropwise. After 10 min, the mixture was poured over ice. The precipitate thus obtained was filtered, washed thoroughly with water, and then dried under vacuum to afford 5.40 g of title compound **5** (yield 90%). ^{1}H NMR ($CDCl_3$): δ 10.32 (s, 2H, CHO), 8.46 (d, 2H), 8.03 (d, 2H), 7.71 (t, 2H). MS (MALDI-TOF): m/z = 240 $[M]^{+\bullet}$. Anal. Calcd for $C_{14}H_8O_2S$: C, 69.98; H, 3.36; S, 13.34. Found: C, 69.60; H, 3.59; S, 12.99.

4,6-Bis-(5,5′-ethoxycarbonyl-4,4′-diethyl-3,3′-dimethyldipyrromethan-5-yl)dibenzothiophene (9). A mixture of 3.20 g of 4,6-diformyldibenzothiophene (**5**) (13.39 mmol) and 9.72 g of ethyl 3-ethyl-4-methyl-1*H*-pyrrole-2-carboxylate (**8**) (60 mmol) was dissolved in 180 mL of hot ethanol. Concentrated hydrochloric acid (3 mL) was then added, and the solution was stirred under reflux for 2 h. The mixture was cooled to room temperature, and the resulting solid was filtered and washed by cold methanol and then dried to give title product **9** (7.00 g, 56%). ^{1}H NMR ($CDCl_3$): δ 8.35 (s, 4H, NH), 8.08 (d, 2H), 7.43 (dd, 2H), 7.03 (d, 2H), 5.66 (s, 2H), 4.22 (q, 8H), 2.71 (q, 8H), 1.81 (s, 12H), 1.28 (t, 12H), 1.05 (t, 12H). MS (MALDI-TOF): m/z = 928.8 $[M]^{+\bullet}$. Anal. Calcd for $C_{54}H_{64}N_4O_8S$: C, 69.80; H, 6.94; N, 6.03; S, 3.45. Found: C, 69.61; H, 6.84; N, 6.20; S, 3.42.

4,6-Bis-(4,4′-diethyl-3,3′-dimethyldipyrromethan-5-yl)dibenzothiophene (12). A suspension of 3.10 g of **9** (3.3 mmol) in diethylene glycol (180 mL) containing NaOH (25.0 g) was heated at 100 °C under N_2 for 1 h 30 min and then at 190 °C for another 1 h 30 min after which the solution was allowed to cool to room temperature. The mixture was poured into ice water (2000 mL), and the resulting solid was filtered, washed with water, and then dried to give compound **12** (2.02 g, 95%). ^{1}H NMR ($CDCl_3$): δ 8.00 (d, 2H), 7.37 (dd, 2H), 7.14 (d, 2H), 6.37 (s, 4H), 5.68 (s, 2H), 2.43 (t, 12H), 1.81 (s, 12H), 1.16 (t, 12H). MS (MALDI-TOF): m/z = 638 $[M]^{+\bullet}$. Anal. Calcd for $C_{42}H_{48}N_4S$: C, 78.71; H, 7.55; N, 8.74; S, 5.00. Found: C, 78.81; H, 7.39; N, 8.53; S, 5.22.

4,6-Bis-(7,13-diethyl-8,12-dimethyl-2,3,17,18-tetraphenylcorrol-10-yl)dibenzothiophene, (BCS)H$_6$ (16). A mixture of 1.00 g (1.5 mmol) of **12** and 1.55 g (6.3 mmol) of 3,4-diphenyl-2-formylpyrrole (**15**) was dissolved in methanol (600 mL). HBr/CH_3CO_2H (5 mL) was then added, and the resulting mixture was stirred at room temperature for 4 h after which $NaHCO_3$ (4.5 g) was added and the mixture stirred again for 10 min. *p*-Chloranil (0.15 g) and hydrazine hydrate (12 mL) were then added, and stirring was continued for 20 min after which the solvent was evaporated under a vacuum and the solid dissolved in CH_2Cl_2. The organic layer was washed with water and dried over $MgSO_4$ and the CH_2Cl_2 evaporated. The solid was chromatographed on basic alumina (grade III, CH_2Cl_2/heptane (60/40) as eluent), and the first violet band was collected to give title corrole dyad **16** (0.340 g, 14%). ^{1}H NMR ($CDCl_3$): δ 9.77 (s, 4H, meso), 8.54 (d, 2H, dibenzothiopheneH), 8.41 (d, 2H, dibenzothiopheneH), 7.92 (dd, 2H, dibenzothiopheneH), 7.86−6.98 (m, 40H, Ph), 3.62 (m, 4H, CH_2−CH_3), 3.47 (m, 4H, CH_2−CH_3), 2.55 (s, 12H, CH_3), 1.35 (t, 12H, CH_2−CH_3), −1.37 (s, 3H, NH), −1.86 (s, 3H, NH). MS (MALDI-TOF): m/z = 1552.87 $[M]^{+\bullet}$. UV−vis (CH_2Cl_2), λ_{max} (nm) ($\epsilon \times 10^{-4}$, mol^{-1} L cm^{-1}): 410 (16.0), 512 (2.2), 567 (2.5), 604 (2.1). Anal. Calcd for $C_{110}H_{88}N_8S$: C, 85.01; H, 5.71; N, 7.21; S, 2.06. Found: C, 84.87; H, 5.65; N, 7.01; S, 1.74.

4,6-Bis-(7,13-diethyl-8,12-dimethyl-2,3,17,18-tetraphenylcorrol-10-yl)dibenzofuran, (BCO)H$_6$ (17). This compound was prepared in 11% yield (0.75 g), as described for **16**, starting from 2.70 g (4.29 mmol) of 4,6-bis-(4,4′-diethyl-3,3′-dimethyldipyrromethan-5-yl)dibenzofuran (**13**) and 4.96 g (20 mmol) of 3,4-diphenyl-2-formylpyrrole (**15**). ^{1}H NMR ($CDCl_3$): δ 9.77 (s, 4H, meso), 8.39 (d, 2H, dibenzofuranH), 8.26 (d, 2H, dibenzofuranH), 8.01 (dd, 2H, dibenzofuranH), 7.90−6.95 (m, 40H, Ph), 3.70 (m, 4H, CH_2−CH_3), 3.50 (m, 4H, CH_2−CH_3), 2.11 (s, 12H, CH_3), 1.22 (t, 12H, CH_2−CH_3), −1.36 (s, 3H, NH), −1.79 (s, 3H, NH). MS (MALDI-TOF): m/z = 1536.69 $[M]^{+\bullet}$. UV−vis (CH_2Cl_2), λ_{max} (nm) ($\epsilon \times 10^{-4}$, mol^{-1} L cm^{-1}): 408 (13.0), 509 (2.2), 567 (2.2), 604 (1.9). Anal. Calcd for $C_{110}H_{88}N_8O$: C, 85.90; H, 5.77; N, 7.29. Found: C, 86.16; H, 5.98; N, 7.38.

4,5-Bis-(7,13-diethyl-8,12-dimethyl-2,3,17,18-tetraphenylcorrol-10-yl)-9,9-dimethylxanthene, (BCX)H$_6$ (18). This compound was prepared in 24% yield (0.59 g), as described for **16**, starting from 1.0 g (1.5 mmol) of 4,5-bis-(4,4′-diethyl-3,3′-dimethyldipyrromethan-5-yl)-9,9-dimethylxanthene (**14**) and 1.84 g (7.4 mmol) of 3,4-diphenyl-2-formylpyrrole (**15**). ^{1}H NMR ($CDCl_3$): δ 9.30 (s, 4H, meso), 7.80 (d, 2H), 7.54−6.96 (m, 44H), 3.47 (s, 6H, Me), 3.31 (m, 8H, CH_2−CH_3), 2.26 (s, 12H, CH_3), 1.54 (t, 12H, CH_2−CH_3), −1.60 (s broad, 3H, NH), −2.10 (s broad,

(19) Barton, D. H. R.; Zard, S. Z. *J. Chem. Soc., Chem. Commun.* **1985**, 1098−1100.
(20) Barton, D. H. R.; Kervagoret, J.; Zard, S. Z. *Tetrahedron* **1990**, *46*, 7587−7598.
(21) Friedman, M. *J. Org. Chem.* **1965**, *30*, 859−863.
(22) Jérôme, F.; Gros, C. P.; Tardieux, C.; Barbe, J.-M.; Guilard, R. *Chem. Commun. (Cambridge)* **1998**, 2007−2008.
(23) Jérôme, F.; Gros, C. P.; Tardieux, C.; Barbe, J.-M.; Guilard, R. *New J. Chem.* **1998**, *22*, 1327−1329.
(24) Chang, C. J.; Deng, Y.; Shi, C.; Chang, C. K.; Anson, F. C.; Nocera, D. G. *Chem. Commun. (Cambridge)* **2000**, 1355−1356.

3H, NH). MS (MALDI-TOF): m/z = 1580 $[M]^{+\bullet}$. UV−vis (CH_2Cl_2), λ_{max} (nm) ($\epsilon \times 10^{-4}$, mol^{-1} L cm^{-1}): 409 (11.0), 517 (2.5), 563 (2.4), 606 (2.1). Anal. Calcd for $C_{113}H_{94}N_8O$: C, 85.90; H, 6.00; N, 7.09. Found: C, 85.78; H, 6.24; N, 6.95.

1-Formyl-8-(13, 17-diethyl-2,3,7,8,12,18-hexamethylporphyrin-5-yl)biphenylene (19). A mixture of 3.53 g (15 mmol) of 1,8-diformylbiphenylene and 10.0 g (15 mmol) of a,c-biladiene dihydrobromide was dissolved in 1.3 L of hot absolute ethanol. *p*-Toluenesulfonic acid (18.0 g) in 240 mL of ethanol was slowly added over 12 h, and the mixture was then stirred under reflux for 24 h. The mixture was cooled to room temperature, and the solvent was evaporated under vacuum. The residue was dissolved in dichloromethane, neutralized with a saturated solution of $NaHCO_3$, and then washed thoroughly with water. The organic phase was dried over $MgSO_4$ and filtered, and the solvent was removed in vacuo. The residue so obtained was chromatographed on a silica column (CH_2Cl_2/MeOH 99/1 as eluent). The appropriate eluent (second fraction) was collected, concentrated, and crystallized from CH_2Cl_2/MeOH to yield **19** (4.61 g; 49% yield) as a purple solid. ^{1}H NMR ($CDCl_3$): δ 10.14 (s, 2H, CH), 9.96 (s, 1H, CH), 7.45 (d, 1H, $^3J_{H-H}$ = 7.3 Hz, biphH), 7.28 (dd, 1H, $^3J_{H-H}$ = 6.8 Hz, $^3J_{H-H}$ = 7.3 Hz, biphH), 7.15 (d, 1H, $^3J_{H-H}$ = 6.8 Hz, biphH), 6.95 (dd, 1H, $^3J_{H-H}$ = 3.5 Hz, $^3J_{H-H}$ = 3.9 Hz, biphH), 6.77 (d, 2H, $^3J_{H-H}$ = 3.5 Hz, biphH), 6.61 (s, 1H, CHO), 4.07 (q, 4H, $^3J_{H-H}$ = 7.3 Hz, CH_2−CH_3), 3.62 (s, 6H, CH_3), 3.53 (s, 6H, CH_3), 3.02 (s, 6H, CH_3), 1.84 (t, 6H, $^3J_{H-H}$ = 7.3 Hz, CH_2−CH_3), −3.21 (s, 1H, NH), −3.36 (s, 1H, NH). MS (EI): m/z = 628 $[M]^{+\bullet}$. IR (KBr) ν cm^{-1}: 2963 (CH), 2924 (CH), 2865 (CH), 1690 (C═O). UV−vis (CH_2Cl_2), λ_{max} (nm) ($\epsilon \times 10^{-4}$, mol^{-1} L cm^{-1}): 404 (17.6), 503 (2.4), 535 (1.7), 572 (1.7), 624 (1.0). Anal. Calcd for $C_{43}H_{40}N_4O\cdot H_2O$: C, 79.85; H, 6.54; N, 8.66. Found: C, 79.72; H, 6.63; N, 8.83.

4-Formyl-6-(13,17-diethyl-2, 3, 7, 8, 12, 18-hexamethylporphyrin-5-yl)dibenzofuran (20). This compound was prepared in 27% yield (1.14 g), as described for **19**, starting from **6** (1.49 mg, 6.64 mmol). ^{1}H NMR ($CDCl_3$): δ 10.22 (s, 2H, CH), 10.04 (s, 1H, CH), 9.93 (s, 1H, CHO), 8.43 (dd, 1H, $^3J_{H-H}$ = 7.7 Hz, $^4J_{H-H}$ = 1.3 Hz), 8.42 (dd, 1H, $^3J_{H-H}$ = 7.7 Hz, $^4J_{H-H}$ = 1.3 Hz), 8.05 (dd, 1H, $^3J_{H-H}$ = 7.7 Hz, $^4J_{H-H}$ = 1.3 Hz), 7.97 (dd, 1H, $^3J_{H-H}$ = 7.7 Hz, $^4J_{H-H}$ = 1.3 Hz), 7.81 (t, 1H, $^3J_{H-H}$ = 7.7 Hz), 7.54 (t, 1H, $^3J_{H-H}$ = 7.7 Hz), 4.12 (q, 4H, $^3J_{H-H}$ = 7.5 Hz, CH_2−CH_3), 3.67 (s, 6H, CH_3), 3.55 (s, 6H, CH_3), 2.33 (s, 6H, CH_3), 1.94 (t, 6H, $^3J_{H-H}$ = 7.5 Hz, CH_2−CH_3), −3.03 (s, 1H, NH), −3.24 (s, 1H, NH). MS (MALDI-TOF): m/z = 645 $[M]^{+\bullet}$. UV−vis (CH_2Cl_2), λ_{max} (nm) ($\epsilon \times 10^{-4}$, mol^{-1} L cm^{-1}): 402 (17.6), 501 (1.5), 534 (0.8), 570 (0.7), 623 (0.3). Anal. Calcd for $C_{43}H_{40}N_4O_2$: C, 80.10; H, 6.25; N, 8.69. Found: C, 80.33; H, 6.48; N, 8.47.

8-[(5,5′-Diethoxycarbonyl-3,3′,4,4′-tetramethyl-2,2′-dipyrryl)-methyl]-1-(13,17-diethyl-2,3,7,8,12,18-hexamethylporphyrin-5-yl)biphenylene (22). Under nitrogen, a mixture of 1.10 g of biphenylenyl porphyrin (**19**) (1.75 mmol) and 0.64 g of 5-ethoxycarbonyl-3,4-dimethylpyrrole (**21**) (3.85 mmol) was dissolved in 200 mL of hot ethanol. *p*-Toluenesulfonic acid (1.8 g) was then added, and the mixture was stirred under reflux for 4 h. The mixture was cooled to room temperature and the solvent removed under vacuum. The residue so obtained was dissolved in dichloromethane and washed with water until a neutral pH was obtained. The organic layers were dried over $MgSO_4$, filtered, and removed under vacuum. After crystallization from CH_2Cl_2/MeOH, title compound **22** was isolated in 86% yield (1.47 g, 1.51 mmol) as purple crystals. ^{1}H NMR (C_6D_6): δ 10.10 (s, 2H, CH), 9.93 (s, 1H, CH), 7.25 (dd, 1H, $^3J_{H-H}$ = 6.3 Hz, $^3J_{H-H}$ = 7.3 Hz, biphH), 7.10 (d, 1H, $^3J_{H-H}$ = 7.3 Hz, biphH), 6.80 (d, 1H, $^3J_{H-H}$ = 6.3 Hz, biphH), 6.70 (d, 1H, biphH), 6.63 (dd, 1H, $^3J_{H-H}$ = 8.3 Hz, biphH), 5.78 (d, 1H, $^3J_{H-H}$ = 8.3 Hz, biphH), 5.28 (s, 1H, CH), 4.29 (q, 4H, $^3J_{H-H}$ = 7.3 Hz, CH_2−CH_3), 4.06 (q, 4H, $^3J_{H-H}$ = 6.8 Hz, CH_2−CH_3), 3.63 (s, 6H, CH_3), 3.46 (s, 6H, CH_3), 2.96 (s, 6H, CH_3), 2.26 (s, 6H, CH_3), 1.86 (t, 6H, $^3J_{H-H}$ = 7.3 Hz, CH_2−CH_3), 1.24 (s, 6H, CH_3), 1.17 (t, 6H, $^3J_{H-H}$ = 6.8 Hz, CH_2−CH_3), −1.34 (s, 1H, NH), −3.39 ppm (s, 1H, NH). MS (EI): m/z = 944 $[M]^{+\bullet}$. IR (KBr) ν cm^{-1}: 3445 (NH), 3277 (NH), 2963 (CH), 2926 (CH), 2868 (CH), 1681 (C═O). UV−vis (CH_2Cl_2), λ_{max}, nm ($\epsilon \times 10^{-4}$ mol^{-1} L cm^{-1}): 407 (14.8), 502 (1.9), 538 (1.3), 571 (1.2), 624 (0.8). Anal. Calcd for $C_{61}H_{64}N_6O_4\cdot H_2O$: C, 76.05; H, 6.91; N, 8.73. Found: C, 76.25; H, 7.08; N, 8.44.

4-[(5,5′-Diethoxycarbonyl-3,3′,4,4′-tetramethyl-2,2′-dipyrryl)-methyl]-6-(13,17-diethyl-2,3,7,8,12,18-hexamethylporphyrin-5-yl)dibenzofuran (23). This compound was prepared in 85% yield (1.55 g), as described for **22**, starting from **20** (1.22 mg, 1.89 mmol). ^{1}H NMR ($CDCl_3$): δ 10.22 (s, 2H, CH), 10.04 (s, 1H, CH), 8.40 (d, 1H, $^3J_{H-H}$ = 7.8 Hz), 8.16 (d, 1H, $^3J_{H-H}$ = 7.8 Hz), 7.86 (d, 1H, $^3J_{H-H}$ = 7.6 Hz), 7.73 (t, 1H, $^3J_{H-H}$ = 7.6 Hz), 7.44 (t, 1H, $^3J_{H-H}$ = 7.8 Hz), 7.14 (d, 1H, $^3J_{H-H}$ = 7.6 Hz), 5.42 (s, 1H, CH), 4.12 (q, 4H, CH_2−CH_3, $^3J_{H-H}$ = 7.8 Hz), 4.01 (q, 4H, $^3J_{H-H}$ = 7.0 Hz, CH_2−CH_3), 3.69 (s, 6H, CH_3), 3.52 (s, 6H, CH_3), 2.19 (s, 6H, CH_3), 1.93 (t, 6H, $^3J_{H-H}$ = 7.8 Hz, CH_2−CH_3), 1.91 (s, 6H, CH_3), 1.10 (t, 6H, $^3J_{H-H}$ = 7.0 Hz, CH_2−CH_3), 0.89 (s, 6H, CH_3), −3.07 (s, 1H, NH), −3.24 ppm (s, 1H, NH). MS (MALDI-TOF): m/z = 961 $[M]^{+\bullet}$. UV−vis (CH_2Cl_2), λ_{max} (nm) ($\epsilon \times 10^{-4}$, mol^{-1} L cm^{-1}): 403 (17.7), 501 (1.5), 534 (0.7), 571 (0.6), 624 (0.3). Anal. Calcd for $C_{61}H_{64}N_6O_5$: C, 76.22; H, 6.71; N, 8.74. Found: C, 76.09; H, 6.48; N, 9.03.

8-[(3,3′,4,4′-Dimethyl-2,2′-dipyrryl)methyl]-1-(13,17-diethyl-2,3,7,8,12,18-hexamethylporphyrin-5-yl)biphenylene (24). Under nitrogen, a suspension of 1.47 g of **22** (1.51 mmol) in diethylene glycol (100 mL) containing NaOH (4.0 g) was heated at 100 °C for 1 h 30 min and then at 190 °C for another 1 h 30 min. The reaction mixture was then allowed to cool to room temperature and poured into ice water (1.5 L). The resulting solid was filtered, washed thoroughly with water, and then dried under vacuum to give title product **24** in 85% yield (1.03 g; 1.28 mmol). ^{1}H NMR (C_6D_6): δ 10.22 (s, 2H, CH), 10.05 (s, 1H, CH), 7.55 (d, 1H, biphH), 6.81 (m, 2H, biphH), 6.57 (d, 1H, $^3J_{H-H}$ = 6.3 Hz, biphH), 6.42 (dd, 1H, $^3J_{H-H}$ = 7.8 Hz, $^3J_{H-H}$ = 7.3 Hz, biphH), 6.08 (d, 1H, $^3J_{H-H}$ = 7.8 Hz, biphH), 5.24 (s, 2H, CH), 4.63 (s, 1H, CH), 3.84 (q, 4H, $^3J_{H-H}$ = 7.3 Hz, CH_2−CH_3), 3.52 (s, 6H, CH_3), 3.40 (s, 6H, CH_3), 3.13 (s, 6H, CH_3), 2.31 (s, 6H, CH_3), 1.76 (t, 6H, $^3J_{H-H}$ = 7.3 Hz, CH_2−CH_3), 1.33 (s, 6H, CH_3), −2.62 (s, 1H, NH), −2.68 (s, 1H, NH). MS (EI): m/z = 800 $[M]^{+\bullet}$. IR (KBr) ν cm^{-1}: 3442 (NH), 2961 (CH), 2925 (CH), 2867 (CH). UV−vis (CH_2Cl_2), λ_{max} (nm) ($\epsilon \times 10^{-4}$, mol^{-1} L cm^{-1}): 405 (7.6), 503 (0.8), 536 (0.5), 572 (0.4), 625 (0.3). Anal. Calcd for $C_{55}H_{56}N_6\cdot H_2O$: C, 80.64; H, 7.14; N, 10.27. Found: C, 80.36; H, 6.95; N, 10.01.

4-[(3,3′,4,4′-Dimethyl-2, 2′-dipyrryl)methyl]-6-(13,17-diethyl-2,3,7,8,12,18-hexamethylporphyrin-5-yl)dibenzofuran (25). This compound was prepared in 87% yield (1.01 g), as described for **24**, starting from **23** (1.39 g, 1.45 mmol). ^{1}H NMR ($CDCl_3$): δ 10.27 (s, 2H, CH), 10.06 (s, 1H, CH), 8.36 (d, 1H, $^3J_{H-H}$ = 7.5 Hz), 8.06 (d, 1H, $^3J_{H-H}$ = 7.5 Hz), 7.90 (d, 1H, $^3J_{H-H}$ = 7.4 Hz), 7.74 (t, 1H, $^3J_{H-H}$ = 7.4 Hz), 7.39 (t, 1H, $^3J_{H-H}$ = 7.5 Hz), 7.31 (d, 1H, $^3J_{H-H}$ = 7.4 Hz), 5.21 (s, 1H, CH), 4.94 (s, 2H), 4.14 (q, 4H, $^3J_{H-H}$ = 7.4 Hz, CH_2−CH_3), 3.72 (s, 6H, CH_3), 3.58 (s, 6H, CH_3), 2.20 (s, 6H, CH_3), 1.93 (t, 6H, $^3J_{H-H}$ = 7.4 Hz, CH_2−CH_3), 1.61 (s, 6H, CH_3), 1.35 (s, 6H, CH_3), −3.05 (s, 1H, NH), −3.20 (s, 1H, NH). MS (MALDI-TOF): m/z = 817 $[M]^{+\bullet}$. UV−vis (CH_2Cl_2), λ_{max} (nm) ($\epsilon \times 10^{-4}$, mol^{-1} L cm^{-1}): 402 (15.7), 501

(1.3), 535 (0.7), 571 (0.6), 624 (0.3). Anal. Calcd for $C_{55}H_{56}N_6O$: C, 80.85; H, 6.91; N, 10.29. Found: C, 80.69; H, 6.72; N, 10.55.

1-(2,3,7,8,12,18-Hexamethyl-13,17-diethylporphyrin-5-yl)-8-(2,3,17,18-tetraphenyl-7,8,12,13-tetramethylcorrol-10-yl)anthracene, (PCA)H$_5$ (33). This compound was prepared as already described.[17,22,23]

1-(2,3,7,8,12,18-Hexamethyl-13,17-diethylporphyrin-5-yl)-8-(2,3,17,18-tetraphenyl-7,8,12,13-tetramethylcorrol-10-yl)biphenylene, (PCB)H$_5$ (28). Under nitrogen, a mixture of 1.26 g of **24** (1.57 mmol) and 0.77 g of 3,4-diphenyl-2-formylpyrrole (**15**) (3.14 mmol) was refluxed in methanol (200 mL). HBr/CH_3CO_2H (10 mL, 33% solution) was then added, and the resulting mixture was refluxed for 15 min. The reaction mixture was then allowed to cool to room temperature after which $NaHCO_3$ (10 g) was added and the mixture stirred again for 10 min. *p*-Chloranil (0.520 g) was then added and the solution stirred for another 10 min. Hydrazine hydrate (18 mL) was then added and stirring continued for 15 min. The porphyrin-corrole precipitates in situ and the solid thus obtained after filtration were further dissolved in CH_2Cl_2. The organic layer was washed with water and dried over $MgSO_4$, and then the solvent was evaporated. The solid was chromatographed on basic alumina (grade III, CH_2Cl_2/heptane 60/40 as eluant), and the first violet band was collected to give title porphyrin-corrole dyad **28** which was recrystallized from CH_2Cl_2/cyclohexane (0.37 g; 0.294 mmol; 19% yield). ^{1}H NMR ($CDCl_3$): δ 9.72 (s, 2H, CH), 8.77 (s, 1H, CH), 7.93 (s, 2H, CH), 7.56 (m, 10H, PhH), 7.52 (d, 1H, $^3J_{H-H}$ = 7.3 Hz, biphH), 7.31 (dd, 1H, $^3J_{H-H}$ = 7.3 Hz, biphH), 7.02 (m, 5H, PhH), 6.91 (m, 4H, biphH), 6.76 (m, 5H, PhH), 4.08 (dq, 2H, CH_AH_B−CH_3), 3.87 (dq, 2H, CH_AH_B−CH_3), 3.25 (s, 6H, CH_3), 3.05 (s, 6H, CH_3), 2.94 (s, 6H, CH_3), 2.79 (s, 6H, CH_3), 2.51 (s, 6H, CH_3), 1.66 (t, 6H, $^3J_{H-H}$ = 7.3 Hz, CH_2−CH_3), −5.82 (s, 1H, NH), −6.20 (s, 1H, NH), −6.34 ppm (s, 3H, NH). MS (LSIMS): *m*/*z* = 1257 $[M + H]^{+\bullet}$. IR (KBr) ν cm^{-1}: 3562 (NH), 3488 (NH), 3437 (NH), 2964 (CH), 2925 (CH), 2860 (CH). UV−vis (CH_2Cl_2), λ_{max} (nm) ($\epsilon \times 10^{-4}$, mol^{-1} L cm^{-1}): 399 (14.7), 501 (3.8), 534 (3.0), 567 (2.8), 620 (2.4). Anal. Calcd for $C_{89}H_{76}N_8 \cdot H_2O$: C, 83.79; H, 6.17; N, 8.79. Found: C, 83.86; H, 6.22; N, 8.71.

4-(2,3,7,8,12,18-Hexamethyl-13,17-diethylporphyrin-5-yl)-6-(2,3,17,18-tetraphenyl-7,8,12,13-tetramethylcorrol-10-yl)dibenzofuran, (PCO)H$_5$ (29). This compound was prepared in 16% yield (290 mg), as described for **28**, starting from **25** (1.22 mg, 1.89 mmol).^{1}H NMR ($CDCl_3$): δ 10.15 (s, 2H, CH), 8.86 (s, 1H, CH), 7.86 (s, 2H, CH), 7.62 (m, 22H), 6.68 (m, 5H, PhH), 4.07 (dq, 2H, CH_AH_B−CH_3), 3.81 (dq, 2H, CH_AH_B−CH_3), 3.34 (s, 6H, CH_3), 3.16 (s, 6H, CH_3), 2.96 (s, 6H, CH_3), 2.38 (s, 6H, CH_3), 2.15 (s, 6H, CH_3), 1.60 (t, 6H, $^3J_{H-H}$ = 7.3 Hz, CH_2−CH_3), −2.12 (s, 1H, NH), −2.60 (s, 1H, NH), −3.84 ppm (s, 3H, NH). MS (MALDI-TOF): *m*/*z* = 1274 $[M]^{+\bullet}$. UV−vis (CH_2Cl_2), λ_{max} (nm) ($\epsilon \times 10^{-4}$, mol^{-1} L cm^{-1}): 401 (22.8), 502 (2.5), 535 (1.6), 571 (1.6), 605 (0.9). Anal. Calcd for $C_{89}H_{76}N_8O \cdot H_2O$: C, 82.76; H, 6.09; N, 8.68. Found: C, 82.57; H, 6.22; N, 8.29.

Cobalt Complexes. 4,6-Bis-[cobalt(III)-7,13-diethyl-8,12-dimethyl-2,3,17,18-tetraphenyl-corrol-10-yl]dibenzothiophene, (BCS)Co$_2$ (30). Cobalt(II) acetate tetrahydrate (100 mg) in 5 mL of absolute methanol was added to a solution of **16** (100 mg, 0.064 mmol) in chloroform (20 mL). The solution was heated to reflux for 20 min, the reaction being monitored by UV−vis spectroscopy. The solvents were then evaporated under vacuum, and the residue was chromatographed on a Florisil column (CH_2Cl_2 + 1% methanol as eluent). The second red band afforded title product **30** which was recrystallized from CH_2Cl_2/methanol (50 mg, 46.7%). MS (MALDI-TOF): *m*/*z* = 1664 $[M]^{+\bullet}$. UV−vis (CH_2Cl_2), λ_{max} (nm) ($\epsilon \times 10^{-4}$, mol^{-1} L cm^{-1}): 405 (16.0), 529 (2.8). Anal. Calcd for $C_{110}H_{82}N_8SCo_2 \cdot 2CH_3OH$: C, 77.76; H, 5.24; N, 6.48. Found: 77.48; H, 4.97; N, 6.11.

4,6-Bis-[cobalt(III)-7,13-diethyl-8,12-dimethyl-2,3,17,18-tetraphenyl-corrol-10-yl]dibenzofuran, (BCO)Co$_2$ (31). This compound was prepared in 25% yield (45 mg), as described for **30**, starting from **17** (170 mg, 0.110 mmol). MS (MALDI-TOF): *m*/*z* = 1648 $[M]^{+\bullet}$. UV−vis (CH_2Cl_2), λ_{max} (nm) ($\epsilon \times 10^{-4}$, mol^{-1} L cm^{-1}): 402 (12.0), 525 (2.8). Anal. Calcd for $C_{110}H_{82}N_8OCo_2 \cdot 2CH_3OH$: C, 78.49; H, 5.29; N, 6.54. Found: C, 78.73; H, 5.44; N, 6.23.

4,5-Bis-[cobalt(III)-7,13-diethyl-8,12-dimethyl-2,3,17,18-tetraphenyl-corrol-10-yl])-9,9-dimethylxanthene, (BCX)Co$_2$ (32). This compound was prepared in 23% yield, as described for **30**, starting from **18** (100 mg, 0.063 mmol). MS (MALDI-TOF): *m*/*z* = 1692 $[M]^{+\bullet}$. UV−vis (CH_2Cl_2), λ_{max} (nm) ($\epsilon \times 10^{-4}$, mol^{-1} L cm^{-1}): 399 (8.5), 525 (3.6). Anal. Calcd for $C_{113}H_{88}N_8OCo_2 \cdot 2CH_3OH$: C, 78.66; H, 5.51; N, 6.38. Found: C, 78.95; H, 5.86; N, 6.43.

1-(Cobalt(II)-2,3,7,8,12,18-hexamethyl-13,17-diethylporphyrin-5-yl)-8-(cobalt(III)-2,3,17,18-tetraphenyl-7,8,12,13-tetramethylcorrol-10-yl)anthracene, (PCA)Co$_2$ (34). This compound was prepared as described in the literature.[17,22,23]

1-(Cobalt(II)-2,3,7,8,12,18-hexamethyl-13,17-diethylporphyrin-5-yl)-8-(cobalt(III)-2,3,17,18-tetraphenyl-7,8,12,13-tetramethylcorrol-10-yl)biphenylene, (PCB)Co$_2$ (35). Under argon, a solution of 0.15 g (0.20 mmol) of porphyrin-corrole dyad **28** and 0.13 g (0.54 mmol) of cobalt(II) acetate tetrahydrate in 10 mL of $CHCl_3$/methanol (70/30) was stirred and refluxed for 1 h 30 min, the metalation reaction being monitored by UV−vis spectroscopy. The solution was then poured in water (100 mL) and extracted with dichloromethane. The combined organic layers were dried over $MgSO_4$. After removal of the solvent in vacuo, the residue so obtained was redissolved in dichloromethane and chromatographed on alumina using CH_2Cl_2/methanol (92/8) as eluent. Title product **35** was isolated in 24% yield (0.065 g; 0.047 mmol) after crystallization from CH_2Cl_2/methanol. MS (MALDI-TOF): *m*/*z* = 1396 $[M]^{+\bullet}$. UV−vis (CH_2Cl_2), λ_{max} (nm) ($\epsilon \times 10^{-4}$, mol^{-1} L cm^{-1}): 393 (10.4), 524 (1.1), 552 (1.2). Anal. Calcd for $C_{89}H_{71}N_8Co_2 \cdot MeOH$: C, 77.08; H, 5.39; N, 7.99. Found: C, 76.86; H, 5.02; N, 7.51.

4-(Cobalt(II)-2,3,7,8,12,18-hexamethyl-13,17-diethylporphyrin-5-yl)-6-(cobalt(III)-2,3,17,18-tetraphenyl-7,8,12,13-tetramethylcorrol-10-yl)dibenzofuran, (PCO)Co$_2$ (36). This compound was prepared in 69% yield, as described for **35**, starting from **29** (200 mg, 0.16 mmol). MS (MALDI-TOF): *m*/*z* = 1386 $[M]^{+\bullet}$. UV−vis (CH_2Cl_2), λ_{max} (nm) ($\epsilon \times 10^{-4}$, mol^{-1} L cm^{-1}): 395 (10.9), 523 (1.3), 555 (1.4). Anal. Calcd for $C_{89}H_{71}N_8OCo_2 \cdot MeOH$: C, 76.21; H, 5.33; N, 7.98. Found: C, 75.80; H, 4.92; N, 7.59.

Equilibrium Constant Measurements. Pyridine and CO binding measurements were carried out at 296 K in CH_2Cl_2, and the reaction was monitored by UV−visible spectroscopy as described in the literature.[15,16] The absorbance was fitted to the Hill equation (eq 1)

$$\log(A_i - A_0)/(A_f - A_i) = \log K + p \log[L] \quad (1)$$

where *p* represents the number of ligands bound to the cobalt center, A_i = absorbance at a specific concentration of ligand, A_0 = initial absorbance where [L] = 0 and A_f = final absorbance where the fully ligated corrole is the only species present.

The application of eq 1 is straightforward but, for the currently investigated biscorroles with weakly or noninteracting macrocyclic units, can give the same slope of p = 1.0 in cases where only one of two metal centers binds an axial ligand or where each Co(III)

center binds a single ligand. The biscorrole complexes investigated in this present paper contain two identical metal centers which are only weakly interacting, and under these conditions, the data from the Hill equation must be combined with spectral data on the Co(III) corrole monomers where the reaction stoichiometry is unambiguous. The binding constants of the biscorroles can then be considered as K_1 and K_2 values of individual cobalt(III) macrocycle where p represents the number of ligands bound to each metal center in a given step.

Results and Discussion

Synthesis. The dialdehyde dibenzothiophene **5** bridge was obtained via a single step in over 80% yield by regioselective dilithiation of the respective unsubstituted heterocyclic spacer (commercially available) and then addition of dry DMF followed by hydrolysis of the intermediate imidate salt. This synthesis is analogous to the one recently reported in the case of dibenzofuran **6** and 9,9-dimethylxanthene **7** derivatives.[10,12,24,25] Condensation of the dialdehyde derivative **5**, with 4.5 equiv of ethyl 3-ethyl-4-methyl-1*H*-pyrrole-2-carboxylate (**8**) in the presence of hydrochloric acid, leads to the respective bisdipyrromethane **9** in over 50% yield (Scheme 2, i).

Saponification, decarboxylation of **9** in NaOH/diethylene glycol was necessary to obtain the α-free bisdipyrromethane **12** (Scheme 2, ii), which was subsequently condensed with 4.2 equiv of 3,4-diphenylpyrrole aldehyde **15** in acidic ethanol to afford the corresponding a,c-biladiene (Scheme 2, iii).[16,22,26] It is noteworthy to point out that attempts to isolate the a,c-biladiene intermediate led to decomposition of the product, and the subsequent cyclization was therefore carried out in situ, buffering the solution with an excess of sodium hydrogen carbonate and using *p*-chloranil as an oxidant (Scheme 2, iv).[16,22,26] Final purification by chromatography on basic alumina afforded the biscorrole $(BCS)H_6$ (**16**) in 14% yield. Bisdipyrromethanes **10** and **11** and the corresponding α-free tetrapyrrole derivatives **13** and **14** were synthesized using a method recently described by Nocera and co-workers in the case of cofacial bisporphyrins.[10,12,24] Starting from α-free bisdipyrromethane **13** and **14**, a similar cyclization procedure was used in order to access the free-base biscorroles $(BCO)H_6$ (**17**) and $(BCX)H_6$ (**18**) in 11% and 24% yield, respectively (Scheme 2).

Using the same experimental procedure as described for the anthracenyl porphyrin-corrole $(PCA)H_5$ (**33**),[17,23,26] the biphenylenyl analogue $(PCB)H_5$ (**28**) was obtained in only three steps starting from monoporphyrin monoaldehyde **19** (Scheme 3). The unsymmetrical porphyrin-dipyrromethane derivative **22** was then isolated in over 80% yield by condensation of **19** with 2.2 equiv of ethyl 3,4-dimethyl-pyrrole-5-carboxylate (**21**) (Scheme 3, i).[8,17] The α-free porphyrin-dipyrromethane intermediate **24** was prepared in 85% yield after subsequent hydrolysis and decarboxylation[27] after which it was reacted with 20 equiv of monoformyl

Scheme 2[a]

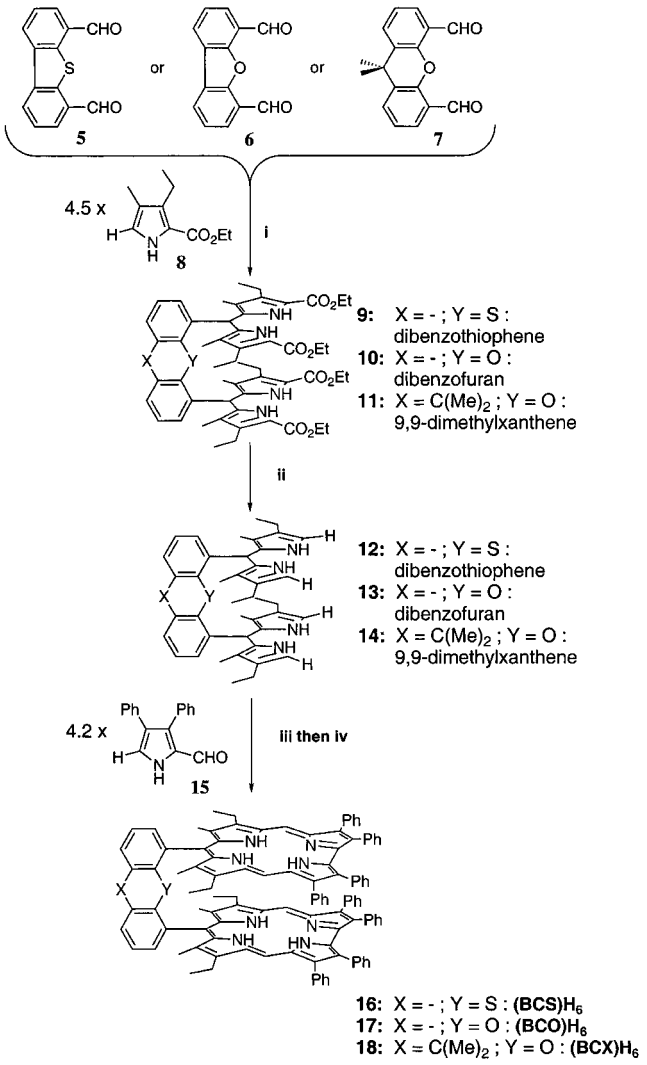

[a] (i) HCl, methanol, 3 h; (ii) NaOH, diethyleneglycol, 100 °C, 1 h 30 min, then 190 °C, 1 h 30 min; (iii) HBr/CH_3CO_2H, 4 h; (iv) $NaHCO_3$, *p*-chloranil, N_2H_4 (50% in water).

pyrrole **15** to give the target porphyrin-a,c-biladiene, **26** (Scheme 3, ii).[17,23,26] In situ addition of sodium hydrogen carbonate and *p*-chloranil followed by addition of 50% hydrazine in water gave **28** as a crude compound after solvent removal (Scheme 3, iii). Compound **28** was finally obtained in 19% yield after column chromatography on alumina. Starting from monoporphyrin derivative **20**, a similar procedure was used in order to access the free-base porphyrin-corrole $(PCO)H_5$ (**29**) in only three steps and in 16% yield (step iii).

Mass Spectrometry. The mass spectral data are given in the Experimental Section. The molecular peak of the free-base biscorrole or the mixed porphyrin-corrole was observed in each case as the most intense peak, and the data agree well with the expected molecular formula. In addition to the systematically observed molecular peak, only minor peaks of very weak intensity were observed, which further proves the stability of the parent compounds.

Electronic Absorption Spectra. UV−vis spectral data of the free-base cofacial biscorroles are summarized in

(25) Hillebrand, S.; Bruckmann, J.; Krüger, C.; Haenel, M. W. *Tetrahedron Lett.* **1995**, *36*, 75−78.
(26) Jérôme, F.; Barbe, J. M.; Gros, C. P.; Guilard, R.; Fischer, J.; Weiss, R. *New J. Chem.* **2001**, *25*, 93−101.
(27) Abdalmuhdi, I.; Chang, C. K. *J. Org. Chem.* **1985**, *50*, 411−413.

Scheme 3[a]

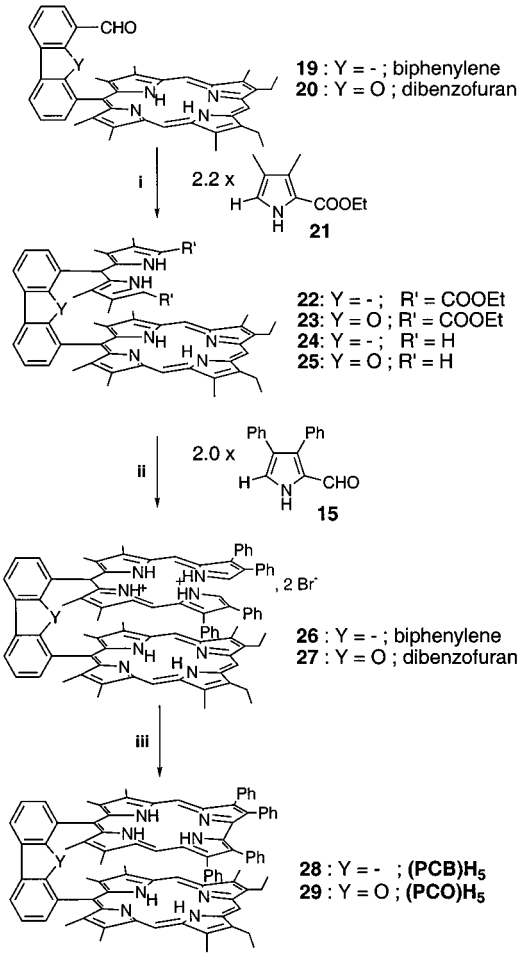

(i) *p*-TsOH, ethanol, 4 h; (ii) NaOH, diethyleneglycol, 100 °C, 1 h 30 min, then 190 °C, 1 h 30 min, then MeOH, HBr, and **15**; (iii) $NaHCO_3$, *p*-chloranil, N_2H_4 (50% in water).

Table 1 which also includes data for the analogous free-base porphyrin-corrole and bisporphyrin complexes as well as analogous monocorrole and monoporphyrin having a similar substitution pattern.

As seen in the table, the Soret and visible bands of the five free-base biscorroles (**1**, **3**, **16**, **17**, and **18**) are all blue-shifted compared to the spectrum of the related free-base monocorrole (7,8,12,13-tetramethyl-2,3,10,17,18-pentaphenylcorrole $(Me_4Ph_5Cor)H_3$: λ_{max} (ϵ, mol^{-1} L cm^{-1}) = 419 (85 000), 567 (15 000), 607 nm (13 000)).[15] A broadening of the Soret band is also observed. The UV−vis absorption spectra of the biscorroles are not a simple superposition of two monocorrole spectra because of the presence of electronic interaction between the two macrocycles, as was previously reported for the Pacman porphyrins.[8] The features of the biscorrole spectra are in good agreement with the cofacial geometry of the two corrole rings as previously confirmed by X-ray structure determination of the trispyridine adduct of the anthracenyl-bridged derivative, $(BCA)Co_2(py)_3$.[16] In contrast, the electronic absorption spectra of the biscorroles have slightly red-shifted Soret and Q-bands as compared to either the bisporphyrin analogue with the same bridge, that is, **16** [λ_{max} = 410 (Soret band), 512, 567, 604 nm] and $(DPS)H_4$ [λ_{max} = 400 (Soret band), 502, 536, 571, 623 nm], or to the well-known free-base Pacman porphyrin $(DPA)H_4$ [λ_{max} = 395 (Soret band), 506, 539, 578, and 631 nm][8] (Table 1). The wavelength differences between the Soret band of the biscorroles $(BCO)H_6$ (**17**) (408 nm) and $(BCX)H_6$ (**18**) (409 nm) and their bisporphyrin analogues, $(DPO)H_4$ (396 nm, Soret band) and $(DPX)H_4$ (389 nm, Soret band), are equal to 12 and 20 nm (where the DPO^{4-} and DPX^{4-} ligands are 4,6-bis[5-(2,8,13,17-tetraethyl-3,7,12,18-tetramethyl-porphyrinyl)]dibenzofuran and 4,5-bis[5-(2,8,13,17-tetraethyl-3,7,12,18-tetramethyl-porphyrinyl)]-9,9-dimethylxanthene, respectively) (see Table 1). The red shift of the corrole absorbances is in accordance with a lower ring current for these bismacrocycles than for the analogous bisporphyrin chromophores.

The electronic absorption spectra of the free-base porphyrin-corrole derivatives $(PCA)H_5$ (**33**) [λ_{max} = 407 (Soret band), 504, 539, 573, 615 nm], $(PCB)H_5$ (**28**) [λ_{max} = 399 (Soret band), 501, 534, 567, 620 nm] and $(PCO)H_5$ (**29**) [λ_{max} = 401 (Soret band), 502, 535, 571, 605 nm] show slightly red-shifted Soret and Q-bands as compared to the well-known free-base "Pacman" porphyrins[28] $(DPA)H_4$ [λ_{max} = 395 (Soret band), 506, 539, 578 and 631 nm], $(DPB)H_4$ [λ_{max} = 379 (Soret band), 511, 540, 580 and 632 nm] and the recently reported $(DPO)H_4$ [λ_{max} = 396 (Soret band), 502, 536, 572 and 624 nm] (Table 1). It should also be noted that wavelength differences between the Soret bands of the free-base porphyrin-corroles $(PCA)H_5$ (**33**) (407 nm), $(PCB)H_5$ (**28**) (399 nm), or $(PCO)H_5$ (**29**) (401 nm) and their biscorrole analogues,[16] $(BCA)H_6$ (**1**) (416 nm, Soret band), $(BCB)H_6$ (**3**) (404 nm, Soret band), and $(BCO)H_6$ (**17**) (408 nm, Soret band), are equal to 9, 5, and 7 nm, respectively. This slight blue shift is in accordance with a larger ring current for the porphyrin chromophore than for the corrole macrocycle. Interestingly, the UV−vis absorption spectra of **28**, **29**, and **33** are not a simple superposition of the porphyrin and corrole chromophore spectra. In particular, the Soret bands of **28**, **29**, and **33** are blue-shifted in comparison with similar bands of the isolated monocorroles having the same substitution pattern (see Table 1); thus, they do not appear as separate absorptions assignable to the individual porphyrin and corrole chromophores. However, it is noteworthy to point out that the absorption is mainly attributable to the porphyrin chromophore (Table 1) which has a higher molar absorptivity [$(Me_6Et_2PhP)H_2$: λ_{max} = 404 nm (ϵ = 186 400 mol^{-1} L cm^{-1}, Soret band)] than the monocorrole [$(Me_4Ph_5Cor)H_3$: λ_{max} = 419 nm (ϵ = 85 000 mol^{-1} L cm^{-1}, Soret band)].

^{1}H NMR Spectra of Free-Base Derivatives. The ^{1}H NMR spectrum of the C_2 symmetric derivative **16** exhibits the characteristic pattern of two corrole units cofacially linked by a dibenzothiophene bridge (see Experimental Section). As expected, the ^{1}H NMR spectra of the free-base biscorroles show the presence of only one resonance in the meso proton region [e.g., δ 9.77 ppm (s, 4H) in the case of $(BCS)H_6$ (**16**)]. Similar NMR features are also observed in the case of the 9,9-dimethylxanthene and dibenzofuran free-base derivatives

(28) Guilard, R.; Lopez, M. A.; Tabard, A.; Richard, P.; Lecomte, C.; Brandès, S.; Hutchison, J. E.; Collman, J. P. *J. Am. Chem. Soc.* **1992**, *114*, 9877−9889.

Table 1. Selected Absorption Maxima (ϵ, CH_2Cl_2) of Free-Base Biscorroles, Porphyrin-Corroles, and Bisporphyrins

		λ_{max}, nm ($\epsilon \times 10^{-4}$ mol^{-1} L cm^{-1})					
macrocycle	compound	Soret band	Q-bands				ref
corrole	$(BCA)H_6$ **(1)**	416 (13.2)			572 (3.5)	608 (2.9)	16
	$(BCB)H_6$ **(3)**	404 (14.1)			578 (4.5)	607 (3.7)	16
	$(BCS)H_6$ **(16)**	410 (16.0)	512 (2.2)		567 (2.5)	604 (2.1)	tw
	$(BCO)H_6$ **(17)**	408 (13.0)	509 (2.2)		567 (2.2)	604 (1.9)	tw
	$(BCX)H_6$ **(18)**	409 (11.0)	517 (2.5)		563 (2.4)	606 (2.1)	tw
	$(Me_4Ph_5Cor)H_3$	419 (8.5)			567 (1.5)	607 (1.3)	15
por-cor[a]	$(PCA)H_5$ **(33)**	407 (15.0)	504 (4.4)	539 (3.8)	573 (3.5)	615 (2.9)	17
	$(PCB)H_5$ **(28)**	399 (14.7)	501 (3.8)	534 (3.0)	567 (2.8)	620 (2.4)	tw
	$(PCO)H_5$ **(29)**	401 (22.8)	502 (2.5)	535 (1.6)	571 (1.6)	605 (0.9)	tw
porphyrin	$(DPA)H_4$	395 (19.1)	506 (1.4)	539 (0.5)	578 (0.6)	631 (0.3)	*b*
	$(DPB)H_4$	379 (17.4)	511 (0.6)	540 (0.2)	580 (0.3)	632 (0.2)	*b*
	$(DPS)H_4$	400 (15.5)	502 (1.4)	536 (0.7)	571 (0.6)	623 (0.3)	38
	$(DPO)H_4$	396 (14.0)	502 (1.2)	536 (0.6)	572 (0.6)	624 (0.5)	38
	$(DPX)H_4$	389 (8.0)	510 (0.5)	544 (0.3)	578 (0.3)	628 (0.1)	38
	$(Me_6Et_2PhP)H_2$	404 (18.6)	501 (1.6)	535 (0.8)	570 (0.7)	623 (0.3)	16

[a] por-cor = porphyrin-corrole. [b] Brandès S. Ph.D. Thesis, Université de Bourgogne, Dijon, France, 1993. tw = this work.

Scheme 4

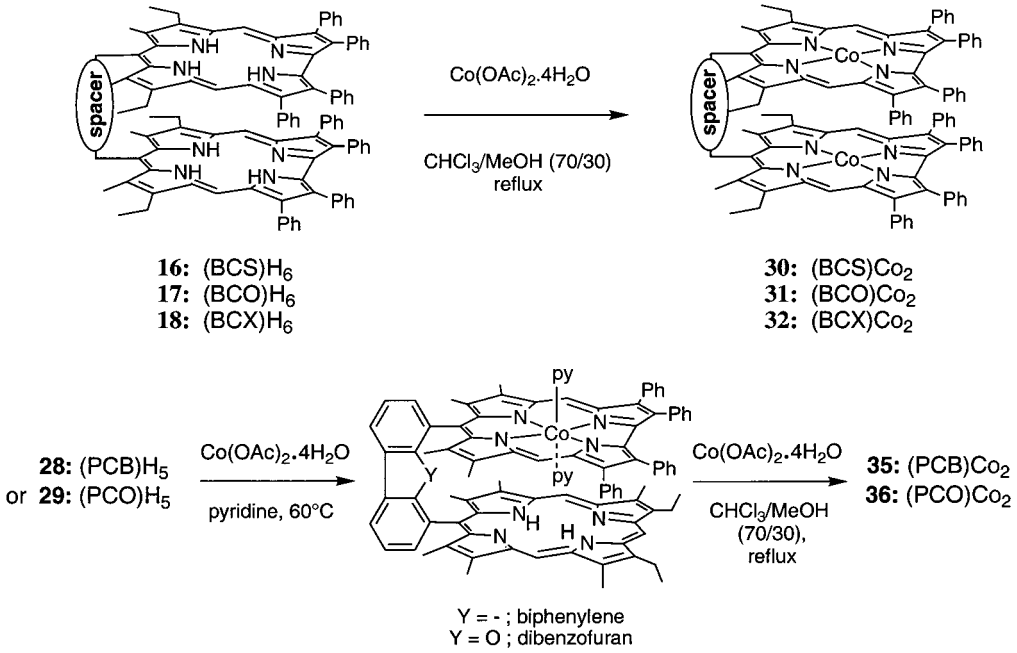

(see Experimental Section). The unsymmetrical free-base porphyrin-corroles $(PCB)H_5$ (**28**) and $(PCO)H_5$ (**29**) (and their respective intermediates) were also characterized by ^{1}H NMR spectroscopy, and these data are given in the Experimental Section. Peak assignments were made on the basis of chemical shifts, multiplicity, integrations, and spectral intercomparisons. As an example, the ^{1}H NMR spectrum of **28** shows well-resolved resonances attributable to both porphyrin and corrole moieties; the meso protons, for example, exhibit a 2:1:2 pattern [δ 7.93 (s, 2H); 8.77 (s, 1H); 9.72 (s, 2H)]. The lack of symmetry is also confirmed by the presence of six CH_3 signals [δ 1.66 (t, 6H); 2.51 (s, 6H); 2.79 (s, 6H); 2.94 (s, 6H); 3.05 (s, 6H); 3.25 (s, 6H)]. The resonances of the internal pyrrolic NH protons are found at higher fields [δ $-$6.34 (s, 3H); $-$6.20 (s, 1H); $-$5.82 (s, 1H)] than for the corresponding monoporphyrin $(Me_6Et_2PhP)H_2$ (δ ca. $-$3.02, $-$3.12) or the monocorrole $(Me_4Ph_5Cor)H_3$ (δ ca. $-$2.70). Similar chemical shifts have also been observed for the free-base porphyrin-corrole anthracenyl derivative $(PCA)H_5$ (**33**).[17,23] In both cases, these are a result of large anisotropic shielding effects that the porphyrin and corrole macrocycles exert on each other when they are held in a close, mutually coplanar arrangement. Such an enhanced chemical shift is also noted in ^{1}H NMR spectra of the biscorroles analogues, $(BCA)H_6$ δ $-$2.83 (4H), $-$3.00 (2H); $(BCB)H_6$ δ $-$5.49 (6H). The two methylene groups of $(PCB)H_5$ are diastereotopic [δ 3.87 (dq, 2H, $CH_AH_B-CH_3$); 4.08 (dq, 2H, $CH_AH_B-CH_3$)]. It is noteworthy to point out that the proton NMR spectrum displays upfield shifts for the NH and meso protons with respect to the corresponding porphyrin and corrole monomers. Such NMR behavior is diagnostic of the close proximity of the porphyrin and the corrole macrocycles to each other.[8,16,17,22,23]

Synthesis of Cobalt Complexes. Standard procedures were employed to metalate the corrole core using cobalt acetate (Scheme 4).[15−17,22,23,29,30] As an example, the free-base biscorrole derivative $(BCS)H_6$ (**16**) was heated under argon in chloroform under reflux with 2.5 equiv of cobalt(II)

acetate tetrahydrate dissolved in a small amount of absolute methanol, the metalation reaction being monitored by UV−vis spectroscopy. Completion of the reaction occurs within 15−20 min as indicated by the disappearance of the absorption at 604 nm and the appearance of a Q-band at about 529 nm, the Soret band being simultaneously slightly red-shifted by about 5 nm. Interestingly, the Soret band of (BCS)Co_2 shifts from 405 nm in CH_2Cl_2 to 415 and 436 nm in neat pyridine, conditions under which the mono- and bis-ligated species are formed (see the following section). A noticeably red to green color change is also observed. After purification, (BCS)Co_2 (**30**) was isolated in over 45% yield. Similar procedures were used to access the two biscobalt derivatives (BCO)Co_2 (**31**) and (BCX)Co_2 (**32**) in 25% and 23% yield, respectively. When dissolved in CH_2Cl_2, the three biscobalt complexes (BCS)Co_2 (**30**), (BCO)Co_2 (**31**), and (BCX)Co_2 (**32**) have well-defined Soret bands at 405 (**30**), 402 (**31**), or 399 nm (**32**) and a single Q-band at 529 (**30**), 525 (**31**), or 525 nm (**32**).

A similar procedure to that previously reported (Scheme 4) was employed to metalate the free-base porphyrin-corroles (PCB)H_5 (**28**) and (PCO)H_5 (**29**) with cobalt. As an example, the porphyrin-corrole (PCB)H_5 (**28**) was first heated in pyridine in the presence of excess of cobalt(II) acetate tetrahydrate. As for the anthracenyl porphyrin-corrole,[17,23] only the corrole ring is metalated at 60 °C, leading to the mixed cobalt corrole/free-base porphyrin complex as seen in Scheme 4. When the temperature is raised to that of pyridine reflux, a metalation of the porphyrin ring occurs. The axial pyridine ligands on the two cobalt centers are readily removed at room temperature under vacuum to give the corresponding unligated complexes.[17,23] The linked porphyrin/corrole biscobalt complexes can be readily obtained starting from the monometalated derivative by using excess cobalt(II) acetate tetrahydrate in a 70/30 chloroform/methanol mixture. It should be noted here that although the final compounds should contain a Co(III) corrole and a Co(II) porphyrin, some oxidation of the porphyrin metal center was observed to occur in solution, thus giving a mixture of two dyads, one of which consisted of a Co(II) porphyrin−Co(III) corrole and other of which contained a Co(III) porphyrin−Co(III) corrole unit. This is discussed in following sections of this paper and was most pronounced in the case of (PCA)Co_2 and (PCB)Co_2 which were easily converted to their singly oxidized Co(III) form, that is, $[(PCA)Co_2]^+$ and $[(PCB)Co_2]^+$ in CH_2Cl_2. On the other hand, almost no oxidation of the cobalt porphyrin unit occurred for the case of (PCO)Co_2 under the same solution conditions.

Electrochemistry and Spectroelectrochemistry of Cobalt Biscorroles. The electrochemistry of (BCS)Co_2, (BCO)Co_2, and (BCX)Co_2 was examined in PhCN, 0.1 M TBAP, and the corresponding potentials are listed in Table 2 which also includes half-wave potentials for the oxidation and reduction of (BCA)Co_2,[16] (BCB)Co_2 ,[16] and (Me_4Ph_5-Cor)Co.[15] The peak currents for reduction of (BCS)Co_2, (BCO)Co_2, and (BCX)Co_2 to their Co(II) form in PhCN are about double the currents for the first oxidation of the same compounds (see Figure 1), and the overall electroreduction behavior is comparable to what was previously described for (BCA)Co_2 under the same solution conditions.[16] The $E_{1/2}$ values for the Co(III)/Co(II) reduction of the three newly synthesized cobalt biscorroles are also close to half-wave potentials for the metal-centered reduction of the corresponding monocorrole, (Me_4Ph_5Cor)Co, which is reversibly reduced at $E_{1/2} = -0.16$ V (see Table 2).

Table 2. Half-wave Potentials (V vs SCE) of Cobalt Corroles in PhCN Containing 0.1 M TBAP

compound	oxidation				reduction	ref
(Me_4Ph_5Cor)Co		0.72	0.47		−0.16	15
(BCS)Co_2	0.97	0.72	0.50	0.24	−0.11	tw
(BCO)Co_2	0.97	0.76	0.48	0.20	−0.16	tw
(BCX)Co_2	1.10	0.76	0.51	0.31	−0.19	tw
(BCA)Co_2		0.89	0.47		−0.23	16
(BCB)Co_2		0.83	0.44	0.27	−0.31[a]	16

[a] A second reversible reduction is seen at −0.60 V; tw = this work.

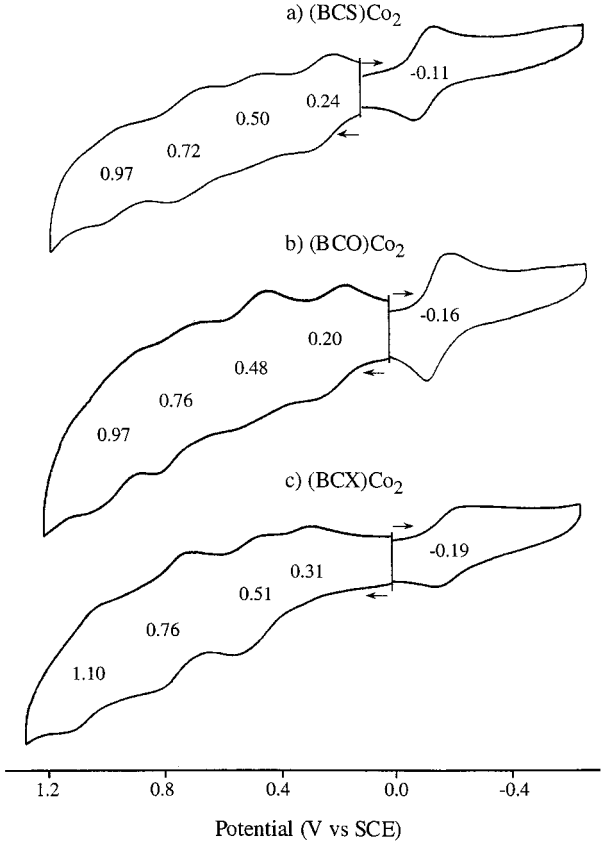

Figure 1. Cyclic voltammograms of (BCS)Co_2, (BCO)Co_2, and (BCX)Co_2 in PhCN, 0.1 M TBAP.

The three biscorroles show similar spectral changes upon electroreduction to the Co(II) complex in a thin-layer cell. An example is given in Figure 2 for the case of (BCS)Co_2 in PhCN containing 0.2 M TBAP. The neutral (BCS)Co_2 complex which is formally a Co(III) derivative has a Soret band at 409 nm and a broad visible band centered at 532 nm (Figure 2a). The spectrum of neutral (BCS)Co_2, which contains two Co(III) macrocycles, is similar to that of the

(29) Conlon, M.; Johnson, A. W.; Overend, W. R.; Rajapaksa, D. *J. Chem. Soc., Perkin Trans. 1* **1973**, 2281−2288.
(30) Paolesse, R.; Licoccia, S.; Fanciullo, M.; Morgante, E.; Boschi, T. *Inorg. Chim. Acta* **1993**, *203*, 107−114.

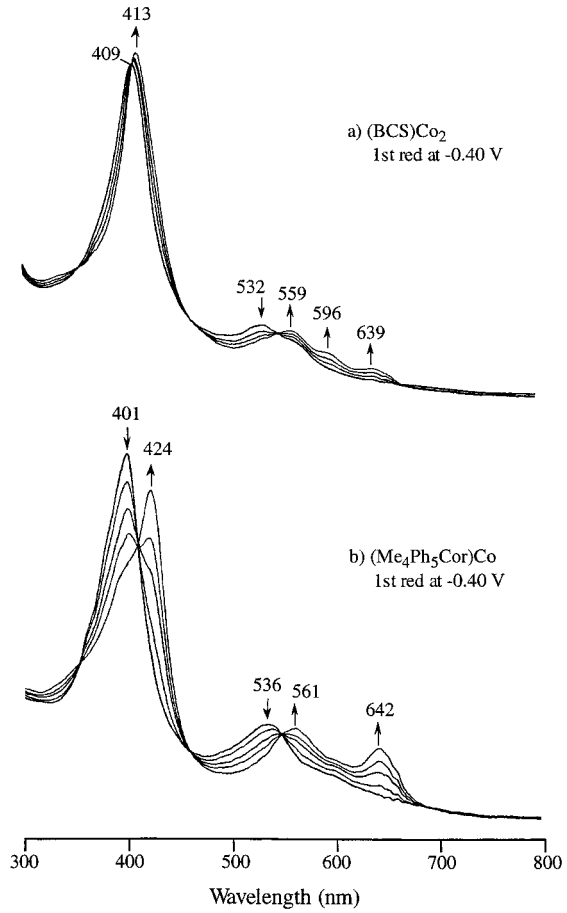

Figure 2. UV−vis spectral changes during thin-layer controlled-potential electrolysis of (a) $(BCS)Co_2$ at −0.40 V and (b) $(Me_4Ph_5Cor)Co$ at −0.40 V in PhCN, 0.2 M TBAP.

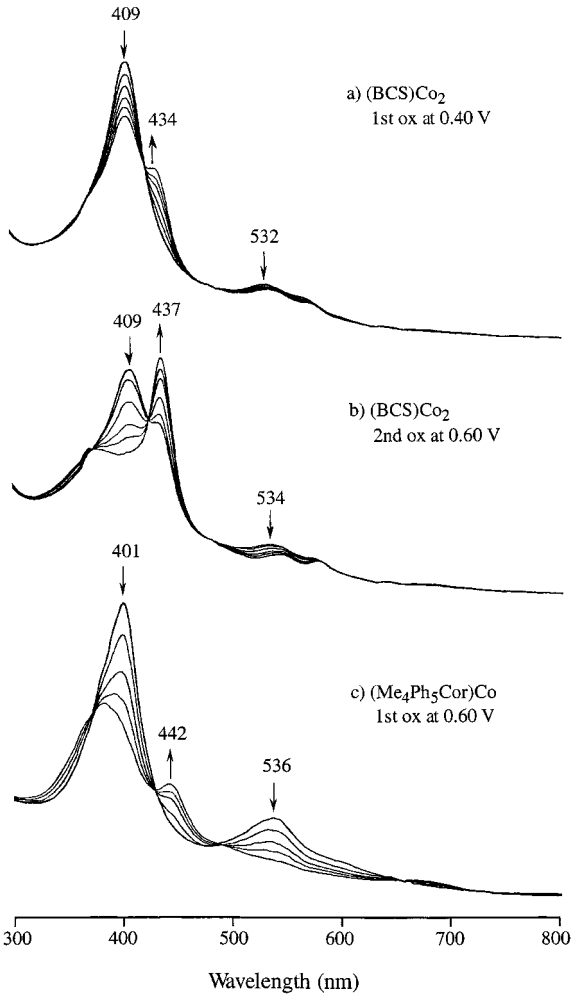

Figure 3. UV−vis spectral changes during thin-layer controlled-potential electrolysis of $(BCS)Co_2$ at 0.40 V (a), 0.60 V (b), and $(Me_4Ph_5Cor)Co$ at 0.60 V (c) in PhCN, 0.2 M TBAP.

neutral monocorrole analogue, $(Me_4Ph_5Cor)Co$, under the same solution conditions (Figure 2b). A reduction of $(BCS)Co_2$ to its Co(II) form at −0.40 V leads to a spectrum with new visible bands at 559, 596, and 639 nm (Figure 2a). A similar metal-centered reduction occurs for (Me_4Ph_5Cor)-Co, and the final product exhibits two new visible bands at 561 and 642 nm after electroreduction. However, the shift in the Soret band upon electroreduction of $(BCS)Co_2$ is smaller than in the case of $(Me_4Ph_5Cor)Co$. The Soret band of $(BCS)Co_2$ shows a small red shift from 409 to 413 nm while $(Me_4Ph_5Cor)Co$ shows a significant red shift from 401 to 424 nm upon electroreduction.

Four oxidations are observed for $(BCO)Co_2$, $(BCX)Co_2$, and $(BCS)Co_2$, and these reactions are proposed to involve the conjugated macrocycle. The half-wave potential for the first oxidation ranges from 0.20 V in the case of $(BCO)Co_2$ to 0.31 V in the case of $(BCX)Co_2$. The second oxidation ranges from $E_{1/2} = 0.48$ V for $(BCO)Co_2$ to 0.51 V for $(BCX)Co_2$ and can be compared to an $E_{1/2} = 0.47$ V for the first oxidation of $(Me_4Ph_5Cor)Co$. The third oxidation of the biscorroles ranges from $E_{1/2} = 0.72$ to 0.76 V while the fourth ranges from 0.97 to 1.10 V.

A comparison of $(BCO)Co_2$, $(BCS)Co_2$, $(BCX)Co_2$, and $(BCA)Co_2$ with the corresponding monocorrole, $(Me_4Ph_5$-$Cor)Co$, clearly indicates that the $E_{1/2}$ values for the second and third oxidations of $(BCO)Co_2$, $(BCS)Co_2$, and $(BCX)Co_2$ are comparable to $E_{1/2}$ values for the first and second oxidations of $(Me_4Ph_5Cor)Co$ and $(BCA)Co_2$. The first two oxidations of $(BCO)Co_2$, $(BCS)Co_2$, and $(BCX)Co_2$ involve a stepwise electron abstraction of one electron from each macrocyclic ring and lead to the formation of monocation radicals and dications.

The spectral changes obtained after the first oxidation of $(BCS)Co_2$ are illustrated in Figure 3a. The Soret band at 409 nm and the broad visible band at 532 nm both decrease with the time of applied potential, and this is accompanied by the appearance of a new Soret band at 434 nm. The second oxidation (Figure 3b) shows a further decrease in intensity of both the 409 and 534 nm bands and is accompanied by an increase of the Soret band intensity at 437 nm. The spectral changes which occur upon the first two oxidations of $(BCS)Co_2$ are both similar to what is seen after the one-electron oxidation of $(Me_4Ph_5Cor)Co$ (Figure 3c).

Pyridine Binding Reactions of Biscorroles. The pyridine binding properties of each cobalt biscorrole were examined in CH_2Cl_2/pyridine mixtures. The UV−vis spectra of the investigated compounds are different in neat pyridine from what is observed in CH_2Cl_2 (see Table 3), thus indicating a coordination of pyridine with the biscorrole complexes.

Table 3. UV−Vis Spectral Data of Cobalt Corroles

compound	λ_{max}, nm ($\epsilon \times 10^{-4}$ mol^{-1} L cm^{-1})						
	CH_2Cl_2 under N_2		pyridine under N_2		CH_2Cl_2 under CO		
$(Me_4Ph_5Cor)Co$[a]	398 (4.5)	529 (1.1)	433 (3.5)	598 (1.7)	407 (3.3)		567 (1.3)
$(BCS)Co_2$	405 (16.0)	529 (2.8)	436 (7.7)	598 (2.5)	408 (11.3)	534 (2.7)	563 (3.2)
$(BCA)Co_2$[b]	402 (9.0)	527 (2.6)	434 (7.6)	598 (3.3)	407 (7.0)	534 (2.3)	567 (2.9)
$(BCO)Co_2$	402 (12.0)	525 (2.8)	434 (6.6)	598 (2.3)	407 (9.7)	533 (2.3)	563 (2.7)
$(BCX)Co_2$	399 (8.5)	525 (3.6)	437 (4.8)	601 (1.9)	406 (7.7)	525 (4.1)	568 (2.9)
$(BCB)Co_2$[b]	390 (8.8)	521 (2.7)	421 (4.5)	601 (1.5)	397 (8.2)	520 (3.2)	564 (2.4)

[a] Data taken from ref 15. [b] Data taken from ref 16.

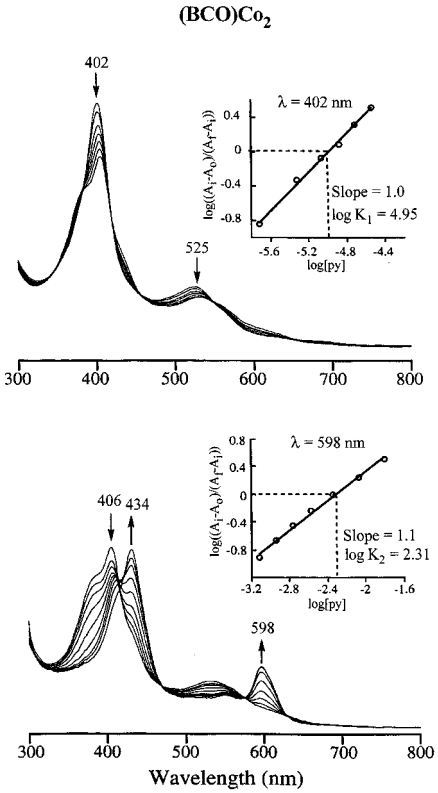

Figure 4. UV−vis spectral changes of 2.0×10^{-6} M $(BCO)Co_2$ during a titration by pyridine in CH_2Cl_2 to give (a) $(BCO)Co_2(py)_2$ and (b) $(BCO)Co_2(py)_3$ in CH_2Cl_2. The inset of each figure shows the Hill plot for each pyridine addition. The pyridine concentration for the plots ranges (a) from 3.0×10^{-6} to 2.5×10^{-5} M and (b) from 6.0×10^{-4} to 0.02 M.

The addition of pyridine to a CH_2Cl_2 solution containing the cobalt biscorrole leads initially to a decrease in intensity of the Soret and visible bands, and this is followed at higher pyridine concentrations by a significant red shift of the Soret band and the appearance of a new intense visible band located at 598−601 nm (see Table 3). These results are similar to what has been reported for $(BCA)Co_2$ [16] and $(BCB)Co_2$.[16] The described spectral changes are associated with the stepwise addition of pyridine to the two cobalt centers of the biscorrole to form five- and six-coordinated complexes. As an example, Figure 4 illustrates the spectral changes for $(BCO)Co_2$ upon increase of the pyridine concentration from 3×10^{-6} to 0.02 M in CH_2Cl_2.

The spectral changes associated with the conversion of $(BCO)Co_2$ to $(BCO)Co_2(py)_2$, a compound which has one bound pyridine per each corrole macrocycle, are shown in Figure 4a. A plot of $\log((A_i - A_o)/(A_f - A_i))$ versus log[py] gives a slope of 1.0 and a binding constant of $\log K_1 = 4.95$,

Table 4. Equilibrium Constants of Biscobalt Corroles and Corrole-Porphyrin Dyads in CH_2Cl_2 at 296 K

compound	pyridine		CO		
	$\log K_1$	$\log K_2$	$P_{1/2}^{CO}$(Torr)	$\log K^c$	ν_{CO} (cm^{-1})
$(Me_4Ph_5Cor)Co$[a]	4.90	2.10	7.1	4.2	2049
$(BCO)Co_2$	4.95	2.31	11.4	4.0	2050
$(BCA)Co_2$[b]	4.84	2.61	15.0	3.9	2047
$(BCX)Co_2$	5.08	2.29	15.8	3.9	2048
$(BCS)Co_2$	4.46	1.63	18.0	3.8	2051
$(BCB)Co_2$[b]	3.14	1.10	31.3	3.6	2046
$(PCO)Co_2$	*d*	*d*	8.9	4.1	2052
$(PCA)Co_2$	*d*	*d*	19.4	3.8	2052
$(PCB)Co_2$	*d*	*d*	48.7	3.4	2042

[a] Ref 15. [b] Ref 16. [c] $[CO] = k_H \cdot P_{co}$, $k_H = 6.7 \times 10^{-3}$ M/atm in CH_2Cl_2, and $K = (P_{1/2}^{CO} \cdot k_H)^{-1}$. [d] Pyridine binding reaction is accompanied by the oxidation of cobalt(II) center in the porphyrin unit which thus limits this measurement.

consistent with coordination of one pyridine molecule to each of the two cobalt centers as shown in eq 2.

$$(BCO)Co_2 + 2py \rightleftharpoons (BCO)Co_2(py)_2 \qquad (2)$$

The spectral changes at higher pyridine concentrations are assigned to the conversion of $(BCO)Co_2(py)_2$ to $(BCO)Co_2(py)_3$ as shown in eq 3 ($\log K_2 = 2.31$). This reaction results in a substantial change in the UV−vis spectra (Figure 4b) where the Hill plot has a slope of 1.1.

$$(BCO)Co_2(py)_2 + py \rightleftharpoons (BCO)Co_2(py)_3 \qquad (3)$$

Similar spectral changes were observed upon pyridine addition to the other investigated compounds, and the values of $\log K_1$ and $\log K_2$ are listed in Table 4. The $\log K_1$ values range from 5.08 in the case of $(BCX)Co_2$ to 3.14 in the case of $(BCB)Co_2$ while $\log K_2$ values range from 2.61 for $(BCA)Co_2$ to 1.10 for $(BCB)Co_2$.

The assignment of three or four bound pyridine molecules to the two cobalt macrocycles is made on the basis of structurally characterized $(BCA)Co_2(py)_3$ [16] combined with spectral comparisons between the different biscorroles and the corresponding monocorrole, $(Me_4Ph_5Cor)Co$, in neat pyridine (Table 3). The visible band at 598−601 nm is an unambiguous "marker band" for assignment of a bispyridine cobalt(III) corrole,[15,16] and the intensity of molar absorptivity (ϵ) of this band therefore should reflect the "relative concentration" or number of six-coordinated pyridine Co(III) centers which are present in the compound as the titration process proceeds.

The $(Me_4Ph_5Cor)Co$ derivative has an ϵ value of 1.7×10^4 for the band at 598 nm in neat pyridine (see Table 3) and has been structurally characterized as

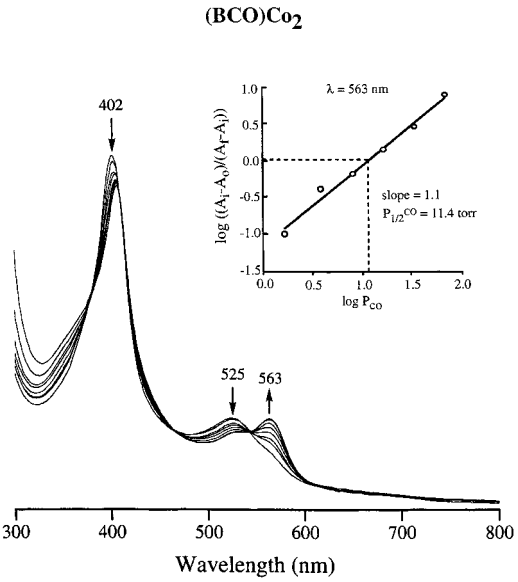

Figure 5. UV−vis spectral changes of 2.5×10^{-6} M $(BCO)Co_2$ during a titration by CO in CH_2Cl_2. The CO partial pressure ranges from 1.6 to 69.0 Torr for the Hill plot.

$(Me_4Ph_5Cor)Co(py)_2$.[15] The 598 nm band of $(BCA)Co_2$ is almost double the ϵ value of the monocorrole (3.3×10^4), thus suggesting that both Co(III) centers of this compound each contain two bound pyridine molecules in neat pyridine and are thus each six-coordinate. This result is consistent with the initial formation of a trispyridine adduct for $(BCA)Co_2$ in CH_2Cl_2 solutions containing 10^{-2} to 10^{-3} M pyridine (1000 times less concentrated than in neat pyridine). It is also consistent with the structure of $(BCA)Co_2(py)_3$ which was obtained for the biscorrole after addition of only a few drops of pyridine to $(BCA)Co_2$ in a $CHCl_3$/MeOH solution.[16] Thus, reaction 4 is proposed to occur upon going from 10^{-3} M pyridine to neat (12 M) pyridine.

$$(BCA)Co_2(py)_3 + py \rightleftharpoons (BCA)Co_2(py)_4 \qquad (4)$$

In contrast to the case of $(BCA)Co_2$, the 598 nm bands of $(BCS)Co_2$ and $(BCO)Co_2$ have molar absorptivities of 2.5×10^4 and 2.3×10^4, respectively (see Table 3), both of which are larger than, but not double, the 1.7×10^4 ϵ value seen for this band in the case of $(Me_4Ph_5Cor)Co(py)_2$. This result indicates that these two biscorroles exist as a mixture of trispyridine and tetrapyridine adducts in neat pyridine but form only the trispyridine complex in CH_2Cl_2 solutions containing 10^{-2} to 10^{-3} M pyridine (the conditions of the pyridine titrations such as the one shown in Figure 4b). Finally, the 601 nm marker band of $(BCX)Co_2$ in neat pyridine has an ϵ value close to that of the monocorrole, and this is consistent with the formation of $(BCX)Co_2(py)_3$, a compound which has two pyridine ligands on one of the cobalt centers and one pyridine molecule on the other, the latter of which shows no UV−vis absorption in the region of 600 nm.

Carbon Monoxide Binding and Electrochemistry of Biscorroles under Different CO Partial Pressures. It has long been known that Co(III) porphyrins can axially bind CO molecules to form five- or six-coordinated complexes.[31−34]

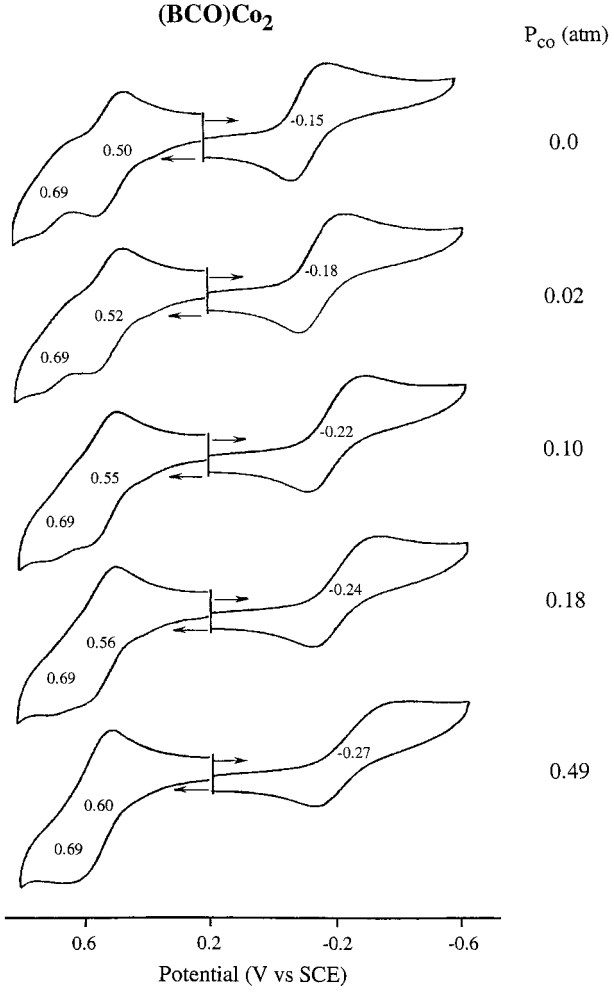

Figure 6. Cyclic voltammograms of $(BCO)Co_2$ under different CO partial pressures in CH_2Cl_2, 0.1 M TBAP.

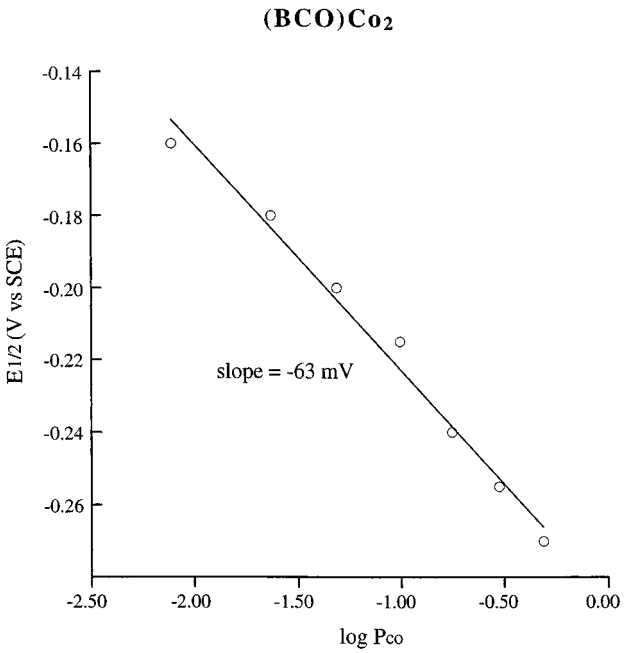

Figure 7. Plot of $E_{1/2}$ for the first reduction of $(BCO)Co_2$ in CH_2Cl_2, 0.1 M TBAP, vs the CO partial pressure (log P_{CO}).

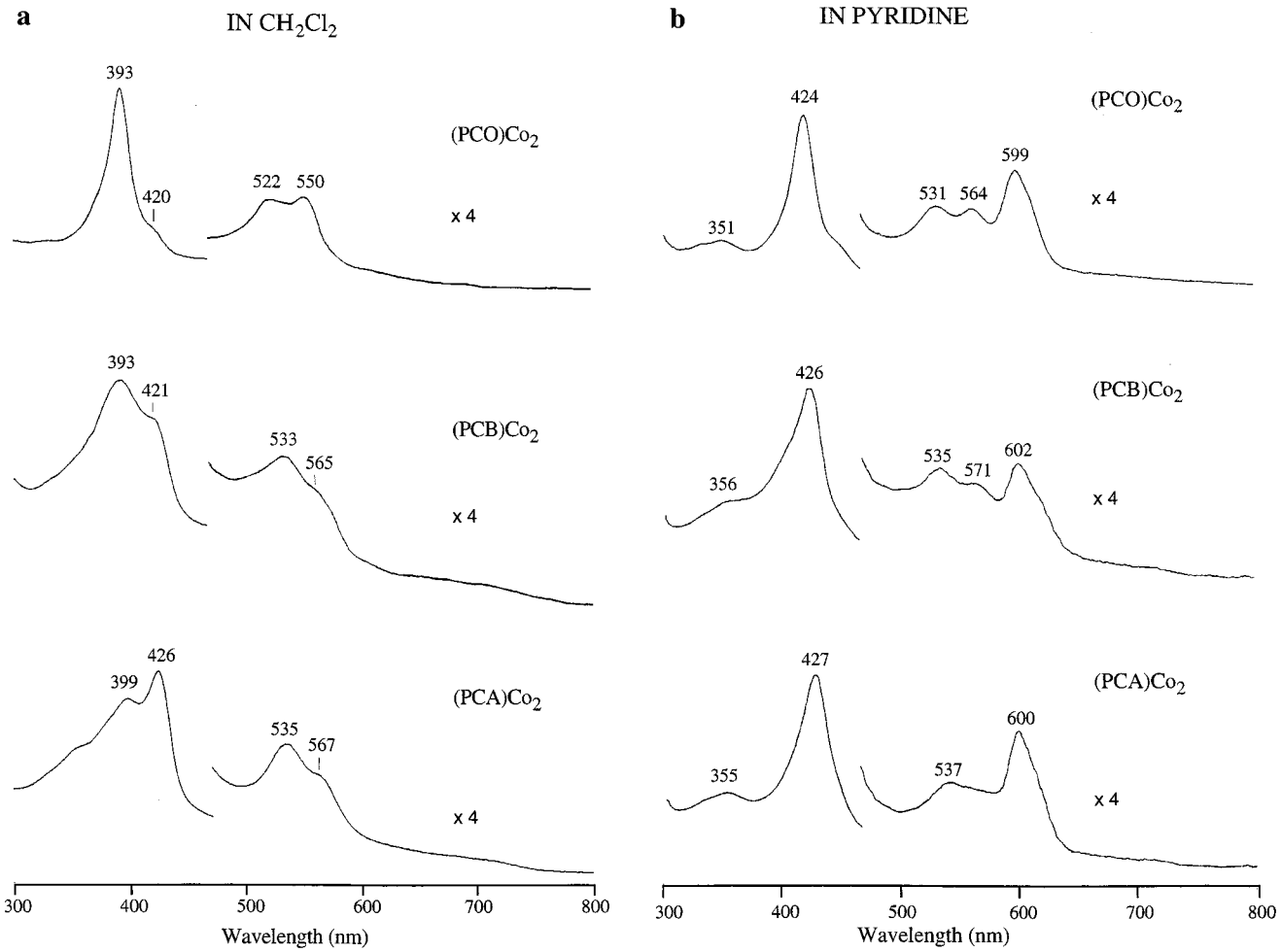

Figure 8. UV−vis spectra of (PCO)Co_2, (PCB)Co_2, and (PCA)Co_2 in (a) CH_2Cl_2 and (b) pyridine.

A similar CO binding reaction occurs for the Co(III) corroles, but only five-coordinate species are seen as was previously demonstrated for a series of mono-[15] and biscorrole[16] complexes. Additional results on CO binding are given in this paper for the newly synthesized cobalt biscorroles possessing different kinds of spacers. Table 3 lists the UV−vis spectral data of each cobalt biscorrole in CH_2Cl_2 under a CO atmosphere. The spectra under CO clearly differ from those under N_2, indicating the existence of CO binding to these complexes.

A quantitative measurement of the CO binding reaction was made by spectrally monitoring the titration of each biscorrole as a function of CO partial pressure. An example of the spectral changes is shown in Figure 5 for the case of (BCO)Co_2. The neutral complex exhibits a Soret band at 402 nm and a visible band at 525 nm in CH_2Cl_2. As CO is introduced into the solution, the intensity of the Soret band slightly decreases, and a new intense visible band appears at 563 nm. The Hill plot (inset of Figure 5) gives a linear relationship with the slope of 1.1, indicating that each cobalt(III) center of the biscorrole coordinates with one and only one CO molecule, thus leading to the formation of five-coordinated complexes as shown in eq 5.

$$(BCO)Co_2 + 2CO \rightleftharpoons (BCO)Co_2(CO)_2 \qquad (5)$$

The CO partial pressure when the binding reaction is half-completed is obtained at $P_{1/2}^{CO} = 11.4$ Torr. This value corresponds to a log $K = 4.0$. Similar CO binding reactions were observed for (BCS)Co_2 and (BCX)Co_2. The measured CO binding constants (log K) are 3.8 for (BCS)Co_2 and 3.9 for (BCX)Co_2 (see Table 4), and both values are comparable to the CO binding constants of (BCA)Co_2 and (BCB)Co_2[16] which have a log $K = 3.9$ and 3.6, respectively. The monocorrole complex, (Me_4Ph_5Cor)Co, has a log $K = 4.2$.[15]

The CO stretching frequencies of each biscorrole were also measured in CH_2Cl_2 under a CO atmosphere. These values range from 2051 cm^{-1} for (BCS)Co_2 to 2046 cm^{-1} for (BCB)Co_2 and can be compared to a $\nu_{CO} = 2049$ cm^{-1} for the monocorrole (Me_4Ph_5Cor)Co[15] (see Table 4).

The CO binding reaction of the cobalt biscorroles was also investigated by electrochemical methods which confirm the binding of one CO to each Co(III) center of the molecules. The formation constants could also be determined from the

(31) Herlinger, A. W.; Brown, T. L. *J. Am. Chem. Soc.* **1971**, *93*, 1790−1791.
(32) Hu, Y.; Han, B. C.; Bao, L. Y.; Mu, X. H.; Kadish, K. M. *Inorg. Chem.* **1991**, *30*, 2444−2446.
(33) Mu, X. H.; Kadish, K. M. *Inorg. Chem.* **1989**, *28*, 3743−3747.
(34) Schmidt, E.; Zhang, H.; Chang, C. K.; Babcock, G. T.; Oertling, W. A. *J. Am. Chem. Soc.* **1996**, *118*, 2954−2961.

electrochemical data, and this is done by recording cyclic voltammograms under different CO partial pressures and then making a plot of $E_{1/2}$ versus the CO partial pressure. An example of one such measurement is shown for the case of $(BCO)Co_2$ in Figures 6 and 7. As seen in these figures, the half-wave potentials of the first reduction shift cathodically upon increase of the CO partial pressure, and the corresponding peak potential separations (ΔE_p) become progressively larger. A plot of $E_{1/2}$ for the first reduction of $(BCO)Co_2(CO)_2$ (which contains one CO group per cobalt center) versus log P_{CO} shows a straight line with a slope of −63 mV, and this value can be compared to a theoretical slope of −59 mV per log P_{CO} for the case where each neutral Co(III) center of the biscorrole binds one CO molecule but dissociates after electroreduction to give a Co(II) corrole which does not bind CO, that is, $[(BCO)Co_2]^{2-}$. From the data in Figure 7, the CO binding constant for neutral $(BCO)Co_2$ is calculated as log $K = 4.4$, which is comparable to the log $K = 4.0$ for CO binding to the same compound as determined by UV−vis spectroscopic techniques (see Table 4). Figure 6 also shows that the first oxidation of $(BCO)Co_2$ shifts in a positive direction (from 0.50 to 0.60 V) with increasing CO partial pressure while the second oxidation remains almost unchanged at $E_{1/2} = 0.69$ V upon going from an N_2 to a CO atmosphere above the solution.

Spectral Characterization of Porphyrin-Corrole Dyads. As indicated earlier, the dyads containing a Co(II) porphyrin and a Co(III) corrole can be easily oxidized at the Co(II) center, and the resulting compounds in CH_2Cl_2 solutions under these conditions will be as a mixture of two dyads containing a Co(III) corrole, one with a Co(II) porphyrin as synthesized and the other with an oxidized Co(III) porphyrin metallomacrocycle. The most air stable dyad is $(PCO)Co_2$ which does not easily interact with O_2 and remains as a pure Co(II) porphyrin/Co(III) corrole dyad in CH_2Cl_2, while the most air unstable dyad is $(PCA)Co_2$ which is substantially converted to $[(PCA)Co_2)]^+$ or possibly $(PCA)Co_2(O_2)$ in CH_2Cl_2. $(PCB)Co_2$ has behavior between that of $(PCO)Co_2$ and $(PCA)Co_2$, and this is shown by UV−vis spectra of the three dyads in CH_2Cl_2 (Figure 8a). As seen in this figure, $(PCO)Co_2$ has a well-defined Co(II) porphyrin spectrum with a Soret band at 393 nm and two visible bands located at 522 and 550 nm. These values are virtually identical to spectral bands of the monoporphyrin, $(Me_6Et_2PhP)Co^{II}$, which is characterized by a Soret band at 396 nm and two visible bands at 522 and 554 nm in CH_2Cl_2.[16] The Co(III) form of the monocorrole, $(Me_6Et_2PhP)Co$, has a Soret band at 426 nm and two visible bands at 538 and 572 nm. Almost the same spectral features are seen for $(PCA)Co_2$ and $(PCB)Co_2$, indicating a conversion of the Co(II) porphyrin to its Co(III) form in solution, that is, $[(PCA)Co_2)]^+$ and $[(PCB)Co_2)]^+$ in Figure 8a.

In contrast to the results in CH_2Cl_2, all three dyads are rapidly converted to their singly oxidized Co(III) porphyrin forms in pyridine, and this is shown in Figure 8b which illustrates the spectra for the three compounds under these solution conditions. There is no evidence for a Co(II) porphyrin in the dyad, and all three complexes have

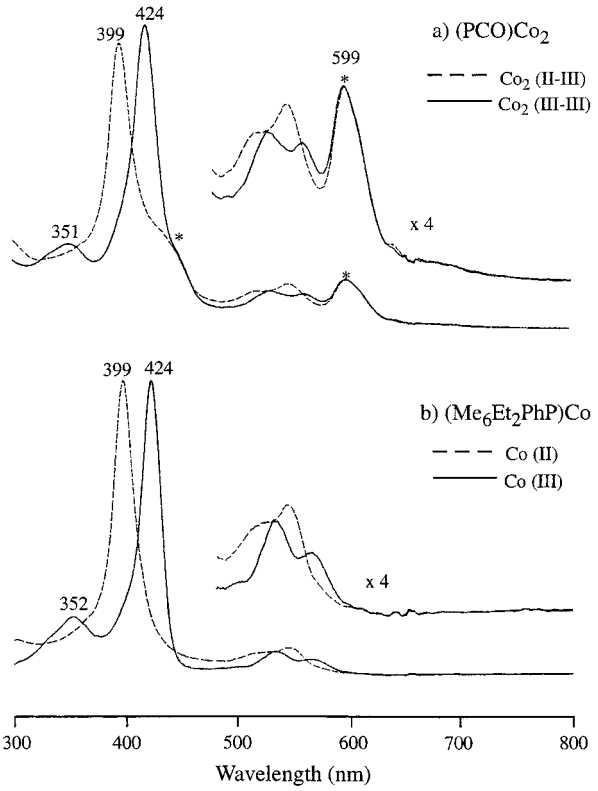

Figure 9. UV−vis spectra of (a) $(PCO)Co_2$ and (b) $(Me_6Et_2PhP)Co$ in neat pyridine as a function of porphyrin oxidation state. The dashed line represents the spectrum of (Por)Co(II)−(Cor)Co(III) or (Por)Co(II) while the solid line represents the spectrum of (Por)Co(III)−(Cor)Co(III) or (Por)Co(III). The bands marked by the star in part (a) are marker bands for the bispyridine Co(III) corrole part of the molecule.

characteristic Co(III) porphyrin UV−vis absorption bands indicating a partial or complete conversion to this oxidation state. The Co(III) monoporphyrin analogue, $[(Me_6Et_2PhP)Co]^+$, has no absorption band in the region of 600 nm, and the intense bands at 599−602 nm for the three dyads in pyridine provide strong evidence for a bispyridine Co(III) corrole part of the molecule as discussed in earlier sections of this manuscript.

Controlled potential electrolysis was used to generate the UV−vis spectra of a pure Co(II) porphyrin/Co(III) corrole or a pure Co(III) porphyrin/Co(III) corrole complex in pyridine. As an example, the spectra of $(PCO)Co_2$ in its neutral (− −) and singly oxidized (—) forms are shown in Figure 9, and a summary of the spectral data for the compounds in each of the two different porphyrin oxidation states is given in Table 5.

The data in Figure 8a indicate that the best dyad to investigate as to its electrochemistry and ligand binding properties is $(PCO)Co_2$ because this porphyrin/corrole complex can be isolated in a stable form containing a Co(II) porphyrin and a Co(III) corrole. The electrochemistry of $(PCO)Co_2$ in PhCN is shown in Figure 10 and consists of seven well-defined oxidation and reduction processes that can be unambiguously assigned to either the porphyrin part of the molecule ($E_{1/2} = 0.96$, 0.39, and −1.02 V) or the corrole part of the molecule ($E_{1/2} = 0.87$, 0.47, −0.19, and −1.64 V). There are also two overlapping oxidations close

Table 5. UV−Vis Spectral Data of Porphyrins and Porphyrin Corroles Having Co(II) and Co(III) Porphyrin Units in Pyridine under N_2[a]

porphyrin oxidation state	compound	λ_{max}, nm ($\epsilon \times 10^{-4}$ mol^{-1} L cm^{-1})				
		Soret region		visible region		
Co(III)	$[(Me_6Et_2PhP)Co]^+$	352 (2.2)	424 (11.9)	535 (1.1)	570 (0.7)	
	$[(PCO)Co_2]^+$	351 (3.0)	424 (11.6)	531 (1.3)	564 (1.2)	599 (1.8)
	$[(PCA)Co_2]^+$	355 (2.2)	427 (5.8)	537 (0.7)	574 (0.7)	600 (1.0)
	$(PCB)Co_2]^+$	356 (2.7)	426 (6.6)	535 (1.0)	571 (0.9)	602 (1.1)
Co(II)	$(Me_6Et_2PhP)Co$		399 (11.8)	524 (1.1)	547 (1.3)	
	$(PCO)Co_2$		399 (11.4)	519 (1.3)	547 (1.5)	599 (1.8)
	$(PCA)Co_2$		402 (5.5)	517 (0.7)	549 (0.8)	600 (1.0)
	$(PCB)Co_2$		402 (5.8)		541 (1.1)	602 (0.7)

[a] Derivatives in the Co(II),Co(III) oxidation state were electrochemically generated by controlled potential reduction in a thin-layer cell, while those with two Co(III) metals were generated by controlled potential oxidation at potentials positive of the Co(III)/Co(II) porphyrin redox process.

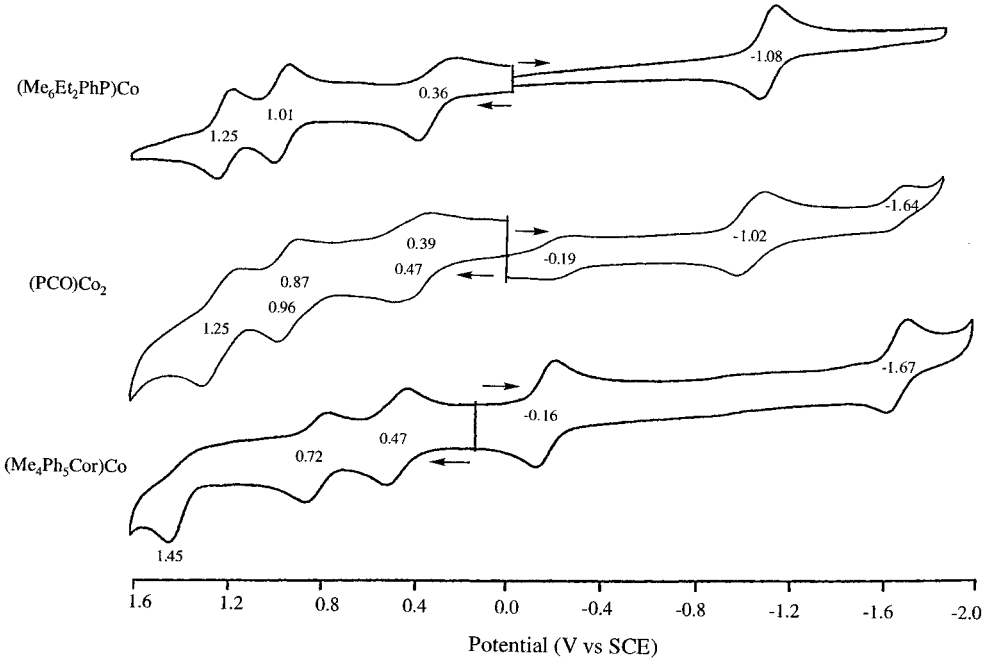

Figure 10. Cyclic voltammograms of $(Me_6Et_2PhP)Co$, $(PCO)Co_2$, and $(Me_4Ph_5Cor)Co$ in PhCN, 0.1 M TBAP.

to 1.25 V, one of which is porphyrin-based and the other of which involves an oxidation of the corrole macrocycle.

The conversion of $(PCO)Co_2$ to $(PCO)Co_2(CO)$ is also well-defined and results in a compound with a ν_{CO} of 2052 cm^{-1} and a log $K = 4.1$ for CO binding to the single corrole macrocycle. There are also well-defined UV−vis changes upon CO addition to the Co(III) center of $(PCO)Co_2$ in CH_2Cl_2. This is shown in Figure 11 where $(PCO)Co_2$ is converted to $(PCO)Co_2(CO)$. It should be noted that there is no evidence for binding of a CO molecule to the porphyrin part of the dyad which would result in a ν_{CO} band greater than 2100 cm^{-1} if the Co(III) porphyrin were present.[35] The ν_{CO} of 2052 cm^{-1} for $(PCO)Co_2(CO)$ is close to the ν_{CO} of $(BCO)Co_2(CO)$ (2050 cm^{-1}) and the other four biscorroles whose data is given in Table 4. The log K_1 for $(PCO)Co_2(CO)$ formation from $(PCO)Co_2$ is also similar to that of $(BCO)Co_2(CO)_2$ as seen in Table 4.

Finally, we must consider the effect of the spacer on the magnitude of K_1 for CO or pyridine binding and how this might be related to $\pi-\pi$ interaction between the two macrocycles. The $\pi-\pi$ interaction between two linked

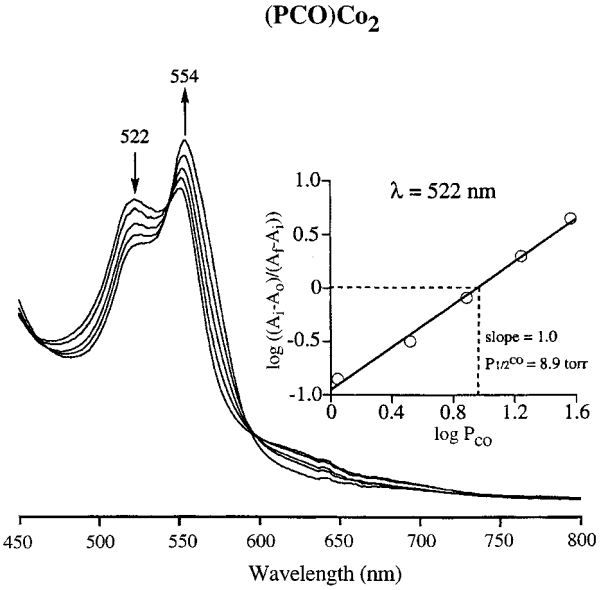

Figure 11. UV−vis spectral changes of 5.0×10^{-6} M $(PCO)Co_2$ during a titration by CO in CH_2Cl_2. The CO partial pressure ranges from 0 to 40.0 Torr for the Hill plot.

macrocycles has been extensively examined in the case of cofacial bisporphyrins[36,37] and depends on the specific bridge

(35) Kadish, K. M.; Shao, J.; Ou, Z.; Comte, C.; Gros, C. P.; Guilard, R. *J. Porphyrins Phthalocyanines* **2000**, *4*, 639−648.

used as a linker. The compounds with shorter bridges generally have decreased cavity sizes and thus an increased $\pi-\pi$ interaction between two porphyrin rings. We would expect that the biscorroles and porphyrin-corroles with shorter spacers would also have the two macrocycles in closer proximity to each other and thus exhibit a greater $\pi-\pi$ interaction which would result in smaller binding constants for the first ligand addition which should occur on the outside of the bismacrocycles.

This is indeed what is observed. The K_1 values for both pyridine and CO binding increase in the following order: $(BCB)Co_2 < (BCS)Co_2 < (BCX)Co_2 \approx (BCA)Co_2 \approx (BCO)Co_2$ for the five biscorrole complexes and $(PCB)Co_2 < (PCA)Co_2 < (PCO)Co_2$ for the three porphyrin-corrole dyads. The two compounds with the shorter biphenylene (B) linkers should have the two macrocycles in the closest proximity to each other if one considers what is known about other free-base bisporphyrins containing the same three spacers as in the PCB, PCA, and PCO complexes. For example, the center to center distances range from a low value of 3.96 Å in the case of the free-base porphyrin dyad $(DPB)H_4$ [38,39] to a larger 4.53 Å in the case of $(DPA)H_4$ [38] and then to 6.90 Å in the case of $(DPO)H_4$,[38,39] which has a flexible spacer and an "open mouth" conformation. Similar distances between the macrocycles are anticipated in the case of the currently studied dyads where the biphenylene linked compounds should have the greatest $\pi-\pi$ interactions between the two macrocycles. At the same time, the biscorrole and porphyrin-corrole dyads with dibenzofuran (O) linkers should have the smallest $\pi-\pi$ interactions, again assuming an "open mouth" conformation due to the high flexibility of the system. As seen in Table 4, these dyads have the largest pyridine and CO binding constants and also have redox potentials which most closely resemble $E_{1/2}$ values for the individual monomacrocycles (see Figure 10). This is consistent with the smallest degree of $\pi-\pi$ interaction between the two macrocycles linked by dibenzofuran and an order of $\pi-\pi$ interaction which increases as follows in the case of the three porphyrin-corrole derivatives: $(PCO)Co_2 < (PCA)CO_2 < (PCB)Co_2$.

Acknowledgment. The support of the Robert A. Welch Foundation (K.M.K., Grant E-680) is gratefully acknowledged. This work was supported by the French Ministry of Research (MENRT), CNRS (UMR 5633). These are gratefully thanked for financial support. The Région Bourgogne and Air Liquide company is acknowledged for scholarships (F.B. and F.J.). The authors are also grateful to M. Soustelle for the synthesis of pyrrole and dipyrromethane precursors.

IC020058+

(36) Le Mest, Y.; L'Her, M.; Hendricks, N. E.; Kim, K.; Collman, J. P. *Inorg. Chem.* **1992**, *31*, 835−847.
(37) Le Mest, Y.; L'Her, M.; Collman, J. P.; Kim, K.; Hendricks, N. H.; Helm, S. *J. Electroanal. Chem.* **1987**, *234*, 277−295.
(38) Bolze F. Ph.D. Thesis, Université de Bourgogne, Dijon, France, 2001.
(39) Bolze, F.; Gros, C. P.; Drouin, M.; Espinosa, E.; Harvey, P. D.; Guilard, R. *J. Organomet. Chem.* **2002**, *643*−*644*, 89−97.